

## Discovery and Optimization of Imidazopyridine-Based Inhibitors of Diacylglycerol Acyltransferase 2 (DGAT2)

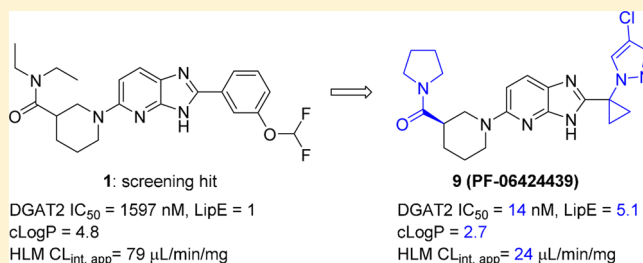
Kentaro Futatsugi,<sup>\*,†</sup> Daniel W. Kung,<sup>\*,||</sup> Suvi T. M. Orr,<sup>||</sup> Shawn Cabral,<sup>||</sup> David Hepworth,<sup>†</sup> Gary Aspnes,<sup>||</sup> Scott Bader,<sup>∇</sup> Jianwei Bian,<sup>||</sup> Markus Boehm,<sup>†</sup> Philip A. Carpino,<sup>†</sup> Steven B. Coffey,<sup>||</sup> Matthew S. Dowling,<sup>||</sup> Michael Herr,<sup>||</sup> Wenhua Jiao,<sup>||</sup> Sophie Y. Lavergne,<sup>||</sup> Qifang Li,<sup>||</sup> Ronald W. Clark,<sup>‡</sup> Derek M. Erion,<sup>‡</sup> Kou Kou,<sup>‡</sup> Kyuha Lee,<sup>⊥</sup> Brandon A. Pabst,<sup>‡</sup> Sylvie M. Perez,<sup>‡</sup> Julie Purkal,<sup>‡</sup> Csilla C. Jorgensen,<sup>#</sup> Theunis C. Goosen,<sup>#</sup> James R. Gosset,<sup>§</sup> Mark Niosi,<sup>#</sup> John C. Pettersen,<sup>○</sup> Jeffrey A. Pfefferkorn,<sup>‡</sup> Kay Ahn,<sup>‡</sup> and Bryan Goodwin<sup>‡</sup>

<sup>†</sup>Worldwide Medicinal Chemistry, <sup>‡</sup>Cardiovascular, Metabolic and Endocrine Diseases Research Unit, and <sup>§</sup>Pharmacokinetics, Dynamics and Metabolism, Pfizer Worldwide Research & Development, Cambridge, Massachusetts 02139, United States

<sup>||</sup>Worldwide Medicinal Chemistry, <sup>⊥</sup>Cardiovascular, Metabolic and Endocrine Diseases Research Unit, <sup>#</sup>Pharmacokinetics, Dynamics and Metabolism, <sup>∇</sup>Pharmaceutical Sciences, and <sup>○</sup>Drug Safety Research & Development, Pfizer Worldwide Research & Development, Groton, Connecticut 06340, United States

### Supporting Information

**ABSTRACT:** The medicinal chemistry and preclinical biology of imidazopyridine-based inhibitors of diacylglycerol acyltransferase 2 (DGAT2) is described. A screening hit **1** with low lipophilic efficiency (LipE) was optimized through two key structural modifications: (1) identification of the pyrrolidine amide group for a significant LipE improvement, and (2) insertion of a sp<sup>3</sup>-hybridized carbon center in the core of the molecule for simultaneous improvement of *N*-glucuronidation metabolic liability and off-target pharmacology. The preclinical candidate **9** (PF-06424439) demonstrated excellent ADMET properties and decreased circulating and hepatic lipids when orally administered to dyslipidemic rodent models.



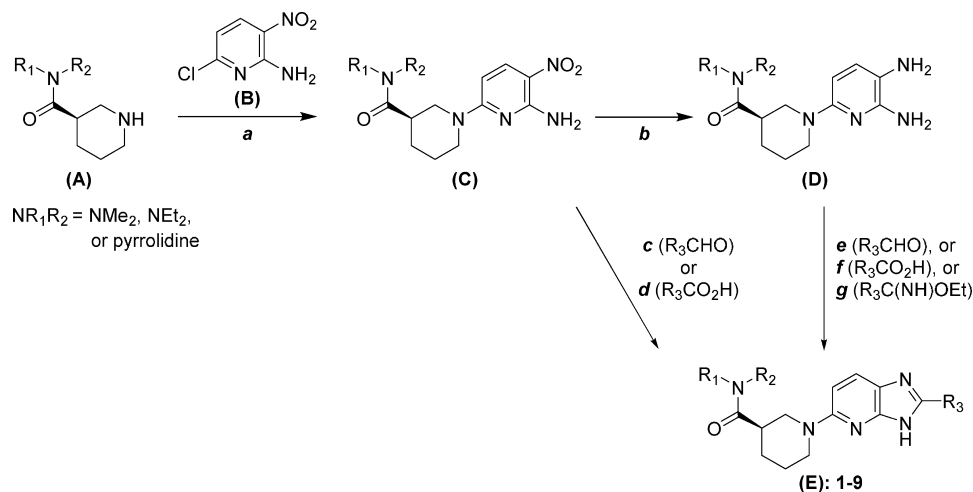
## INTRODUCTION

Globally, 39% of adults are estimated to have hypercholesterolemia.<sup>1</sup> Reduction of low-density lipoprotein (LDL) cholesterol via statin therapy has been demonstrated to decrease adverse cardiovascular events in both the primary and secondary prevention settings.<sup>2</sup> As a class, statins have been effective, but there remains significant residual risk for cardiovascular events in patients unable to achieve LDL treatment target with current therapies.<sup>3</sup> More recently, it has been proposed that plasma triglyceride (TG) levels causally associate with coronary artery disease; however, the cardiovascular benefit of pharmacological TG lowering, in isolation of other lipid parameters, has not been established.<sup>4</sup> Dietary TGs are transported on chylomicrons, whereas TGs released and secreted from the liver are carried on very-low density lipoprotein (VLDL). In addition to the role of VLDL in hepatic TG secretion, VLDL is the primary metabolic precursor of LDL. One potential mechanism to reduce both circulating TG and LDL would be the blockade of hepatic VLDL secretion. However, therapies that directly target this pathway have limited therapeutic utility due to concerns over the accumulation of excess liver fat and gastrointestinal toleration.<sup>5</sup>

Diacylglycerol acyltransferases (DGAT) catalyze the terminal step in the synthesis of triacylglycerol (TG) through the

esterification of diacylglycerol (DAG) with fatty acyl Coenzyme A (CoA).<sup>6</sup> In mammals, two structurally unrelated DGAT enzymes, DGAT1 and DGAT2, have been characterized. DGAT1 is abundantly expressed in the intestine, where it plays a critical role in the absorption of dietary lipid.<sup>7</sup> DGAT2 is found in the liver and adipose tissue and, unlike DGAT1, exhibits exquisite substrate specificity for DAG.<sup>8</sup> Extensive medicinal chemistry efforts have led to the development and characterization of selective small-molecule inhibitors of DGAT1.<sup>9</sup> Although these molecules exhibited an attractive preclinical profile, clinical development has been hindered by significant gastrointestinal side effects.<sup>10,11</sup> Nevertheless, Novartis's DGAT1 inhibitor LCQ908 (pradigastat) remains in phase III trials for familial chylomicronemia syndrome. Targeted disruption of the murine *Dgat2* gene results in postnatal lethality and, as a result, much of our understanding of the physiological function of DGAT2 is derived from preclinical studies using antisense oligonucleotides (ASO) and overexpression.<sup>12</sup> These studies consistently demonstrated that ASO-mediated knockdown of hepatic DGAT2 resulted in decreased VLDL secretion, lower plasma cholesterol and TG

Received: June 27, 2015

Scheme 1. General Synthetic Routes to Compounds 1–9<sup>a</sup>

<sup>a</sup>Conditions: (a) Et<sub>3</sub>N, CH<sub>3</sub>CN, or DMSO, 80–110 °C; (b) H<sub>2</sub>, Pd/C, EtOH, (HCl); (c) R<sub>3</sub>CHO, Na<sub>2</sub>S<sub>2</sub>O<sub>4</sub>, EtOH–H<sub>2</sub>O, 110 °C; (d) (i) H<sub>2</sub>, Pd/C, Boc<sub>2</sub>O, (ii) R<sub>3</sub>CO<sub>2</sub>H, T3P, NMM, THF, reflux, (iii) MsOH, HOAc, then NaOAc; (e) R<sub>3</sub>CHO, sulfur, DMF, toluene, 85 °C; (f) (i) BOP, NMM, DMF, 50 °C, (ii) NaOMe, MeOH, iBuOH, 110 °C; (g) R<sub>3</sub>C(NH)OEt, HOAc, Et<sub>3</sub>N, EtOH, 100 °C.

levels, and reduced hepatic lipid burden.<sup>13</sup> Improved hepatic insulin resistance and glycemic control were also reported.<sup>13a</sup> Although the precise molecular mechanisms underlying these observations are not clear, it was hypothesized that inhibition of DGAT2 led to suppression of de novo lipogenesis and induction of oxidative pathways as a result of a transient increase in lipid intermediates.<sup>13a,c</sup> Thus, the inhibition of DGAT2 is an attractive therapeutic hypothesis which, if successful, would lead to improved plasma lipid profile, decreased hepatic fat accumulation, and improved glycemic control in patients with metabolic disease.

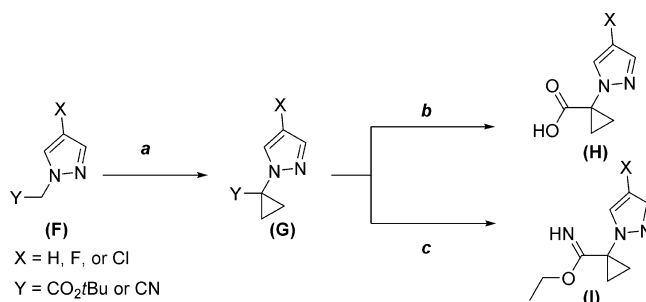
To date, several small-molecule DGAT2 inhibitors have been reported, but most have suffered from weak to modest in vitro potencies, and no in vivo evaluations disclosed.<sup>9b,14,15</sup> We sought to identify an orally bioavailable, potent, and selective small-molecule DGAT2 inhibitor that would (1) allow us to evaluate the physiological function of DGAT2 in vivo in preclinical models and (2) ultimately lead to a candidate with the potential to evaluate the clinical utility of DGAT2 inhibition in patients. Herein we describe the medicinal chemistry efforts to achieve these objectives, culminating in the discovery of the preclinical candidate 9 (PF-06424439).

## CHEMISTRY

The C2-aryl and C2-alkyl imidazopyridines described in this work were synthesized by the general methods shown in Scheme 1. The piperidine-3-carboxamides **A**, readily prepared from *N*-protected piperidine-3-carboxylic acid, were reacted with chloro-nitropyridine **B** under S<sub>N</sub>Ar conditions to provide the diaminonitropyridine **C**. Several methods were used to convert intermediate **C** to the fully functionalized imidazopyridine core **E**. In one step, diaminonitropyridine **C** was transformed directly to imidazopyridines (**R**)-1, (**S**)-1, **2**, and **3** by reductive cyclization with aldehydes R<sub>3</sub>CHO using sodium dithionite.<sup>16</sup> Alternatively, in a multistep sequence, diaminonitropyridine **C** was reduced and monoprotected in situ as a *tert*-butyl carbamate. Amidation with carboxylic acid R<sub>3</sub>CO<sub>2</sub>H, followed by Boc deprotection and cyclization, afforded the imidazopyridine product such as compound **7**. In an alternative two-step sequence, diaminonitropyridine **C** was first reduced to

triaminopyridine **D** by hydrogenation. The free base of **D** was prone to air oxidation, which was mitigated by immediate use of the free base or by isolation of the dihydrochloride salt that was stable upon storage. Imidazopyridine products **E** were formed by reaction of triaminopyridine **D** with either aldehyde,<sup>17</sup> carboxylic acid,<sup>18</sup> or imidate reagents, as shown in Scheme 1. Imidazopyridine **1** was synthesized by cyclization of triaminopyridine **D** with aldehyde R<sub>3</sub>CHO. Imidazopyridine **6** was accessed by treatment of **D** with carboxylic acid R<sub>3</sub>CO<sub>2</sub>H in a two-step amidation–cyclization sequence. Imidazopyridines **5**, **8**, and **9** were prepared by condensation of **D** with imidates R<sub>3</sub>C(NH)OEt.

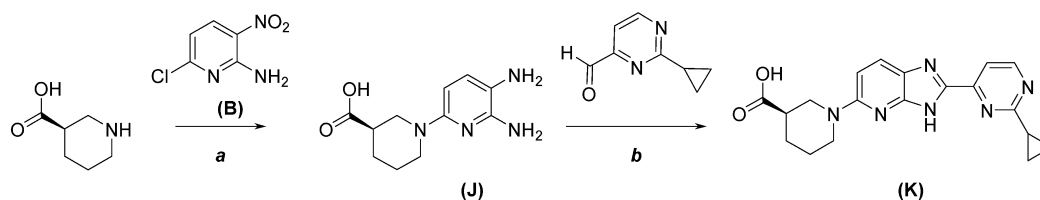
The cyclopropyl-substituted pyrazole carboxylic acid and imidate intermediates used in the synthesis of compounds **7**, **8**, and **9** were prepared as shown in Scheme 2. Bis-alkylation of

Scheme 2. Synthesis of Pyrazole Intermediates<sup>a</sup>

<sup>a</sup>Conditions: (a) for Y = CO<sub>2</sub>tBu, LiHMDS, THF, 1,3,2-dioxathiolane-2,2-dioxide, –78 to 23 °C, or for Y = CN, NaH, 1,2-dibromoethane, DMSO, 0–23 °C; (b) TFA, DCM; (c) sodium metal, EtOH, 70 °C.

the acetate ester or acetonitrile with 1,3,2-dioxathiolane-2,2-dioxide or 1,2-dibromoethane formed the cyclopropyl intermediate **G**.<sup>19</sup> Cleavage of the ester **G** (Y = CO<sub>2</sub>tBu) afforded acid **H**, while imidate **I** was derived from the corresponding nitriles **G** (Y = CN) via sodium ethoxide addition.

Exploration of SAR of the piperidine carboxamide group via parallel synthesis required a change in the order of steps to allow for late-stage amidation of intermediate **K** as shown in

Scheme 3. Synthesis of Carboxylic Acid K for Parallel Synthesis Variation of the Piperidine Amide<sup>a</sup>

<sup>a</sup>Conditions: (a) (i)  $i\text{Pr}_2\text{NEt}$ , DMF, 80 °C, (ii) Zn,  $\text{HCO}_2\text{NH}_4$ , DMF, 45 °C; (b) HOAc, DMF, 60 °C.

**Scheme 3.** In analogous fashion to the routes described in **Scheme 1**, piperidine-3-carboxylic acid was reacted with chloropyridine **B** under  $\text{S}_{\text{N}}\text{Ar}$  conditions, followed by reduction of the nitro group to afford triaminopyridine **J**. Reaction of **J** with the appropriate aldehyde afforded the parallel synthesis substrate **K**. For example, compound **4** was synthesized in a library of amidation products derived from acid **K**.

### IN VITRO PHARMACOLOGY

DGAT2 activity was determined by measuring the incorporation of the [ $1\text{-}^{14}\text{C}$ ]decanoyl moiety into triacylglycerol using [ $1\text{-}^{14}\text{C}$ ]decanoyl-CoA and 1,2-didecanoyl-*sn*-glycerol as substrates. After partitioning by the addition of a phase partition scintillation fluid, the generated product [ $^{14}\text{C}$ ]tridecanoylglycerol was quantified from the upper organic phase. We have utilized a DGAT2 membrane fraction prepared from an Sf9 insect cell expression system as a source of DGAT2 enzyme. In this system, we observed that the host cells possessed an enzyme activity that efficiently hydrolyzed [ $^{14}\text{C}$ ]acyl-CoA to [ $^{14}\text{C}$ ]fatty acid and CoA. The generated [ $^{14}\text{C}$ ]fatty acid products readily partitioned into the organic layer along with the DGAT2 reaction product [ $^{14}\text{C}$ ]triacylglycerol, which precluded accurate quantitation of DGAT2 activity without further separation steps. Furthermore, under these conditions, [ $^{14}\text{C}$ ]acyl-CoA substrate concentration decreases as the reaction proceeds. Others have previously observed the hydrolyzing activity while running DGAT1–2 and MGAT1–3 assays, where the quantitation of the TG/DAG products was achieved after a separation step, typically by TLC.<sup>20</sup>

We have speculated that this acyl-CoA hydrolytic enzyme activity is likely due to thioesterase(s) which belong(s) to the serine hydrolase family of enzymes. We therefore assessed a general serine hydrolase inhibitor methyl arachidonyl fluorophosphonate (MAFP) and found that MAFP at 0.1–1  $\mu\text{M}$  indeed inhibited the thioesterase activity completely without affecting DGAT2 activity. As expected, the  $\text{IC}_{50}$  values for DGAT2 inhibitors were not affected by MAFP. Inhibition of this endogenous thioesterase activity by MAFP allowed us to carry out the DGAT2 assay by phase partitioning and quantitation of TG in the upper organic layer without separation steps in a 384-well plate format as described under the **Experimental Section**. Similarly, we have observed that MAFP inhibited endogenous thioesterase activity without affecting DGAT1 and MGAT1–3 activity and thus utilized MAFP in these assays that were used for selectivity assessment of DGAT2 inhibitors. The membranes prepared from Sf9 cell expression system were utilized as sources of these acyltransferases.<sup>21</sup>

Substrate concentrations for acyl-CoA and DAG (or monoacylglycerol (MAG)) in DGAT1–2, and MGAT1–3 assays were established at (or near) the  $K_m$  values for DGAT2

and all other acyltransferase assays. When the  $K_m$  value for DAG (or MAG) was greater than its solubility limit, the highest substrate concentration of the substrate achievable without precipitation was chosen as the final assay condition. Each preparation of the enzyme was titrated, and the reaction time course was analyzed to ensure that the final reaction conditions were chosen from the linear range of the reaction.

Mechanistic studies revealed that some but not all DGAT2 inhibitors from the imidazopyridine series described herein are reversible, time-dependent inhibitors. These inhibitors bind to DGAT2 through a rapid equilibrium followed by a much slower isomerization of the initial enzyme–inhibitor complex to form a much higher affinity complex. On the basis of this mechanism,  $\text{IC}_{50}$  values were determined after a 120 min preincubation of DGAT2 with inhibitors.<sup>21</sup>

### RESULTS AND DISCUSSION

Initial hit compound **1** (**Figure 1**) was identified through screening a subset of the Pfizer compound collection.

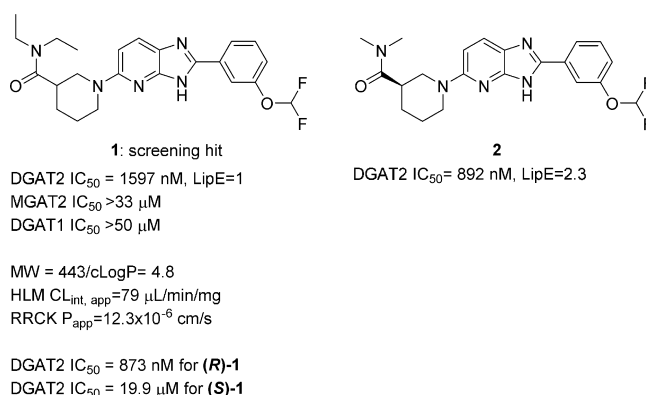
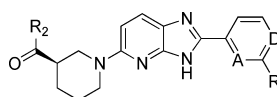


**Figure 1.** Profile of screening hit **1** and its truncated analogue **2**.

Compound **1** is a reversible inhibitor of DGAT2<sup>21</sup> and showed modest inhibitory potency for DGAT2, with >10-fold selectivity against MGAT2 and DGAT1. Compound **1** exhibited a less than ideal profile as a starting point, with low lipophilic efficiency (LipE =  $\text{pIC}_{50} - \text{cLogP}$ )<sup>22</sup> and high intrinsic clearance in human liver microsomes (HLM), which was consistent with its high lipophilicity (cLogP = 4.8). However, we hypothesized that a compound design strategy emphasizing physicochemical property improvement, coupled to the large chemical space that could be rapidly accessed from the parallel synthesis-enabled scaffold of **1**, would provide an opportunity for rapid hit optimization. Initial structure–activity relationship (SAR) examinations around **1** revealed that (1) removal of the diethyl amide group on the piperidine ring of **1** led to a significant decrease in potency (data not shown), (2) the (*R*)-enantiomer was the eutomer (DGAT2  $\text{IC}_{50}$  = 873 nM

Table 1. Optimization of Compound 2



Cpd	R <sub>1</sub>	A/D	R <sub>2</sub>	DGAT2 IC <sub>50</sub> (nM) <sup>a</sup>	cLogP	LipE	HLM CL <sub>int,app</sub> (μL/min/mg)
2	OCF <sub>2</sub> H	CH/CH		892 <sup>c</sup>	3.7	2.3	22
3	cPr	CH/CH		608 (293–1262)	4.2	2.0	39
4 <sup>b</sup>	cPr	N/N		1471 (660–3279)	2.1	3.8	10
5	cPr	N/N		18 (15–22)	2.4	5.4	50

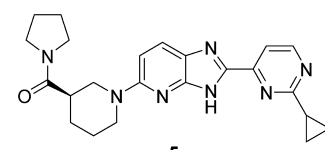
<sup>a</sup>Human DGAT2 potency reported as the geometric mean of at least three replicates. Numbers in parentheses are 95% confidence interval. <sup>b</sup>Tested as a formate salt. <sup>c</sup>Data of single experiment.

and 19.9 μM for (R)-1 and (S)-1, respectively), and (3) truncation of the diethyl amide to the corresponding dimethyl amide retained potency (2, Figure 1). On the basis of this SAR, the initial medicinal chemistry effort focused on decreasing the lipophilicity of the most hydrophobic region of 2, the *meta*-OCF<sub>2</sub>H-Ph group.

Table 1 summarizes key SAR from the optimization of compound 2. With slightly increased lipophilicity and comparable potency, the *meta*-cyclopropyl-phenyl analogue 3 possessed similar LipE to that of 2. Examination of heteroaryl analogues of the phenyl ring showed that pyrimidine 4, although somewhat less potent than the phenyl analogue 3, provided a substantial reduction in lipophilicity; its significantly improved LipE reflected a good balance of properties and, importantly, the decreased lipophilicity also translated to improved HLM stability. Compound 4, with its relatively low cLogP, became the next starting point for LipE-guided potency optimization. Considering the importance of the carboxamide group for DGAT2 inhibition in this series (vide supra), it was reasoned that small changes in the amide substituents might significantly influence DGAT2 potency. Maintaining the cyclopropyl-pyrimidine of 4 and limiting cLogP < 3 in order to minimize possible increases in clearance, a small set of amide groups was examined. Among those tested, tertiary amides exhibited the highest potency; cyclic derivatives such as pyrrolidine amide 5 demonstrated substantially improved LipE and absolute potency. Compound 5 showed higher metabolic turnover in HLM relative to 4, however, likely due to increase in lipophilicity from 4 and the introduction of the site of metabolism (pyrrolidine ring). On the basis of its good physicochemical properties and attractive potency, compound 5 was selected for further characterization (Table 2).

Compound 5 exhibited an excellent selectivity profile against other acyltransferases (MGAT2, DGAT1). Broader off-target selectivity screening (CEREP panel, PDE selectivity panel)

Table 2. Profile of Compound 5



MW 417, eLogD <sup>23</sup> 2.4, TPSA 91	
DGAT2 IC <sub>50</sub> ± SEM (nM) <sup>a</sup>	18 ± 2
MGAT2/DGAT1 IC <sub>50</sub> (μM) <sup>a</sup>	>40/>50
HLM CL <sub>int,app</sub> (μL/min/mg)	50
Human hepatocytes CL <sub>int,app</sub> (μL/min/million cells)	71
HLM-UGT CL <sub>int,app</sub> (μL/min/mg)	316
off-target activities >50% at 10 μM (CEREP panel/PDE selectivity panel)	8 hits <sup>b</sup>

<sup>a</sup>Human DGAT2, MGAT2, or DGAT1 potency reported as the geometric mean of at least three replicates. SEM = standard error of the mean. <sup>b</sup>Adenosine-A2A K<sub>i</sub> = 3700 nM; muscarinic M1 K<sub>i</sub> = 4500 nM; histamine H1 agonism, 50% effect at 10 μM; alpha 1a agonism, 62% effect at 10 μM. PDE IC<sub>50</sub>s (nM): 3300 (1B), 1980 (5A), 9410 (6A), 1490 (11).

revealed several weak, but undesired off-target activities, notably in a subset of PDEs (Table 2, footnote b). Metabolically, high turnover in both HLM and human hepatocytes was also observed. To determine the contribution of glucuronidation pathway to overall metabolism of 5, follow-up studies using alamethicin activated HLM with UDP-glucuronosyltransferase (UGT) enzyme cofactors (HLM-UGT CL<sub>int</sub> assay)<sup>24</sup> were employed. It was revealed that 5 was rapidly metabolized in the presence of the UGT cofactor uridine diphosphate-glucuronic acid (UDPGA), which implicated an unanticipated phase II metabolism via presumed *N*-glucuronidation<sup>25</sup> on the imidazopyridine ring (HLM-UGT CL<sub>int,app</sub> = 316 μL/min/mg, Table 2).

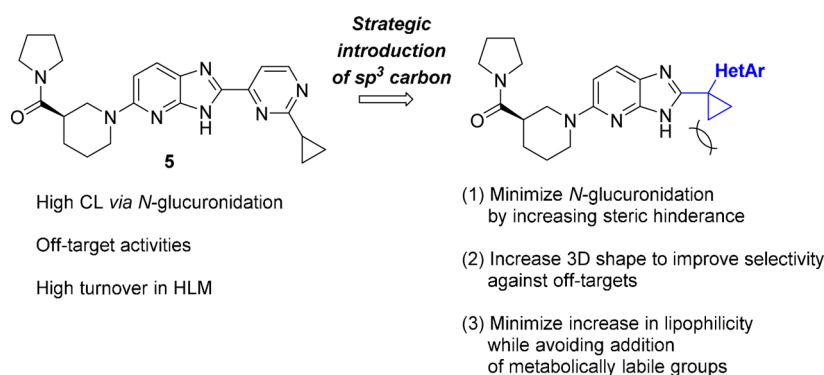


**Figure 2.** Design strategy for simultaneous optimization of off-target selectivity and *N*-glucuronidation.

**Table 3.** Optimization of Heteroaromatic Groups in Imidazopyridines with Cyclopropyl Spacers

cpd	HetAr	DGAT2 $IC_{50}$ (nM) <sup>a</sup>	cLogP	LipE	HLM $CL_{int,app}$ ( $\mu$ L/min/mg)	HLM-UGT $CL_{int,app}$ ( $\mu$ L/min/mg)
5		18 (15 – 22)	2.4	5.4	50	316
6		165 (108 – 251)	2.3	4.5	26	<1.9
7		243 (188 – 315)	1.9	4.7	<9	N/D <sup>b</sup>
8		81 (72 – 92)	2.1	4.9	<9	<1.9
9		14 (12 – 16)	2.7	5.1	24	<1.9

<sup>a</sup>Human DGAT2 potency reported as the geometric mean of at least three replicates. Numbers in parentheses are 95% confidence interval. <sup>b</sup>Not determined.

To address both the off-target pharmacology and the *N*-glucuronidation liabilities, a single design strategy was employed by increasing three-dimensional shape of the core of the molecule through introduction of an  $sp^3$ -hybridized carbon center (Figure 2). The added three dimensionality was expected to improve off-target selectivity.<sup>26</sup> With regard to metabolism, we hypothesized that increased steric bulk around the likely sites of *N*-glucuronidation (imidazole *N*–H) might diminish interaction with the UGT enzyme(s).<sup>27</sup> It was deemed important to limit the increase in lipophilicity from the  $sp^3$ -center in order to mitigate increased CYP-mediated metabolism. To balance the desired steric bulk with undesired lipophilicity (and to avoid introducing another stereocenter),

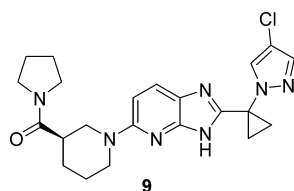
cyclopropyl was selected as the spacer between the imidazopyridine and the terminal heteroaromatic ring (Figure 2, highlighted in blue). It was envisioned that variation of the heteroaromatic ring would enable the fine-tuning of physicochemical properties and potency. The SAR for selected compounds within the scope of this design hypothesis is summarized in Table 3.

Among initial heteroaromatic derivatives synthesized, the 2-pyridyl analogue 6 showed no detectable turnover in the HLM-UGT  $CL_{int}$  assay, providing validation for the hypothesis of mitigating *N*-glucuronidation by means of three-dimensionality from the cyclopropyl ring. Pyridine 6 showed a 10-fold decrease in DGAT2 potency but moderate clearance in HLM. The *N*-

linked pyrazole analogue **7** was examined as a structural mimic of the 2-pyridyl analogue **6**, with the expectation that its lower lipophilicity would diminish metabolic turnover in HLM. While the potency of pyrazole **7** did not increase as compared to that of pyridine **6**, its improved LipE, low metabolic turnover in HLM, and relatively low lipophilicity prompted us to examine further substitution on the pyrazole. By focusing on substituents that were likely not to be metabolically labile, we hoped to achieve a >10-fold increase in potency while maintaining an acceptable clearance profile. The fluoro- and chloro-pyrazole analogues **8** and **9** exhibited promising combinations of potency and clearance properties. Chloro-pyrazole **9** possessed the highest potency and LipE among analogues tested while maintaining an acceptable clearance profile in HLM and no measurable turnover in the HLM-UGT  $CL_{int}$  assay.<sup>28</sup> Furthermore, compound **9** did not show any significant off-target activity (<50% effect at 10  $\mu$ M) in the CEREP and PDE selectivity panels, confirming the improvement in promiscuity over the prototype **5**. On the basis of positive attributes mentioned above, compound **9** was further profiled in a series of in vitro assays (Table 4).

**Table 4. Summary of Pharmacology and ADME Data for Compound 9**

MW 440, eLogD <sup>23</sup> 2.2, TPSA 83, pK <sub>a</sub> = 4.1 (basic)	
DGAT2 IC <sub>50</sub> ± SEM (nM) (human/rat/dog)	14 ± 1/38 ± 4/16 ± 1
IC <sub>50</sub> (MGAT1–3, DGAT1) ( $\mu$ M)	>50
fresh human hepatocytes IC <sub>50</sub> ± SEM (nM)	1.3 ± 0.5
CEREP panel	<50% at 10 $\mu$ M
HLM CL <sub>int,app</sub> ( $\mu$ L/min/mg)	24
HLM-UGT CL <sub>int,app</sub> ( $\mu$ L/min/mg)	<1.9
human hepatocytes CL <sub>int,app</sub> ( $\mu$ L/min/million cells)	9.1
RRCK P <sub>app</sub> (cm/s)	33.9 × 10 <sup>-6</sup>
thermodynamic solubility (methanesulfonic acid salt)	0.83 mg/mL
FaSSIF (simulated fasted intestinal fluid with bile salts)	
f <sub>up</sub> (human/rat/dog)	0.154/0.117/0.111



Compound **9** inhibited DGAT2 of different species (human, rat, and dog) with similar potency. Among related acyltransferases, no significant inhibition was observed for compound **9** (up to 50  $\mu$ M) against human MGAT2 or MGAT3, DGAT1, or mouse MGAT1, indicating a high selectivity (>2000-fold) against these enzymes. To determine the effect of **9** on TG synthesis in a cellular system, freshly isolated human hepatocytes were cultured in the presence of [1,3-<sup>14</sup>C]-glycerol and the incorporation of radiolabel into TG was monitored using TLC. To monitor DGAT2 activity, a selective DGAT1 inhibitor {*trans*-4-[4-(4-amino-5-oxo-7,8-dihydropyrimido[5,4-*f*][1,4]oxazepin-6(*5H*)-yl)phenyl]cyclohexyl}acetic acid (PF-04620110, 3  $\mu$ M)<sup>29</sup> was added to completely inhibit endogenous DGAT1 activity. In this cell-based system, DGAT1 appeared to play a redundant role and it was not possible to consistently measure DGAT2 activity in the absence

of a DGAT1 inhibitor. The DGAT1 inhibitor (PF-04620110) reduced [<sup>14</sup>C]glycerol incorporation into TG by ~30%. The addition of **9** on top of a DGAT1 inhibitor further lowered TG synthesis by ~40–50% (data not shown). In this assay, compound **9** showed potent inhibitory activity with an IC<sub>50</sub> of 1.3 nM.

A crystalline form of **9** was obtained as a methanesulfonic acid salt (basic pK<sub>a</sub> of **9** = 4.1), which exhibited excellent thermodynamic solubility in FaSSIF (simulated fasted intestinal fluid with bile salts) (0.83 mg/mL). The high solubility, coupled with reasonable metabolic stability and high passive permeability, prompted evaluation of the in vivo pharmacokinetic properties of **9** (Table 5). Compound **9** showed moderate

**Table 5. In Vivo Pharmacokinetic Profile of 9 in Rat and Dog<sup>a</sup>**

species	dose (mg/kg)	route	t <sub>1/2</sub> (h)	CL <sub>p</sub> (mL/min/kg)	Vd <sub>ss</sub> (L/kg)	F (%)
rat	1 <sup>b,f</sup>	iv	1.39	18.4	1.16	NA <sup>h</sup>
rat	5 <sup>c,g</sup>	po	2.37	NA	NA	~100
dog	1 <sup>e,f</sup>	iv	1.15	18.4	2.01	NA
dog	5 <sup>d,g</sup>	po	1.65	NA	NA	~100

<sup>a</sup>For rat PK studies, male Wistar-Han rats were utilized. For dog PK studies, male beagle dogs were used. All data reported here are means of two experiments. <sup>b</sup>Vehicle was 10% DMSO/90% of 40% SBEDC in water. <sup>c</sup>Vehicle was 0.5% methylcellulose/0.1% Tween 80. <sup>d</sup>Vehicle was 0.5% methylcellulose. <sup>e</sup>Vehicle was 10% PEG200/90% of 12% SBEDC in water. <sup>f</sup>Free base of **9** was dosed. <sup>g</sup>Crystalline, methanesulfonic acid salt of **9** was dosed. <sup>h</sup>NA = not applicable.

clearance in rat and dog following intravenous administration, consistent with the moderate metabolic stability observed in liver microsomes of the respective species (CL<sub>int,app</sub> [ $\mu$ L/min/mg] in rat and dog liver microsomes = 20 and 26, respectively). Moderate steady-state volume of distribution (Vd<sub>ss</sub>) resulted in a short-to-moderate half-life. High solubility and high passive permeability of **9** translated into high oral bioavailability (F ~ 100%) in both species.

On the basis of its excellent in vitro pharmacological profile and favorable in vivo pharmacokinetic properties, compound **9** was selected to evaluate the acute effects of DGAT2 inhibition on hepatic secretion of TGs in male Sprague–Dawley rats (Figure 3). Dose-dependent reductions in plasma TG were observed after an oral administration of **9**, with a maximal effect of >50% reduction in plasma TG relative to vehicle control. The magnitude of the effect on plasma TG reduction correlated with the plasma free drug levels of **9** (Figure 3). In contrast to isolated human hepatocytes (vide supra), the observed changes in TGs were achieved in the absence of DGAT1 inhibitor in this setting.

To evaluate the effects of DGAT2 inhibition in a dyslipidemia rodent model, low-density lipoprotein receptor knockout mice (*Ldlr*<sup>-/-</sup>) were treated with 60 mg/kg/day (administered as 30 mg/kg BID) **9** for 3 days. When maintained on standard laboratory chow, *Ldlr*<sup>-/-</sup> mice exhibit elevated plasma triglycerides and cholesterol, however, when fed a high-fat, high-cholesterol diet (HFHC), these animals develop pronounced hyperlipidemia with total plasma cholesterol levels in excess of 1500 mg/dL (Figure 4). Treatment of *Ldlr*<sup>-/-</sup> mice on a HFHC diet with **9** resulted in 61% (*p* < 0.001) and 34% (*p* < 0.001) reductions in plasma TG and cholesterol levels, respectively (Figure 4A,B). The HFHC diet-induced increase in circulating TG levels was completely

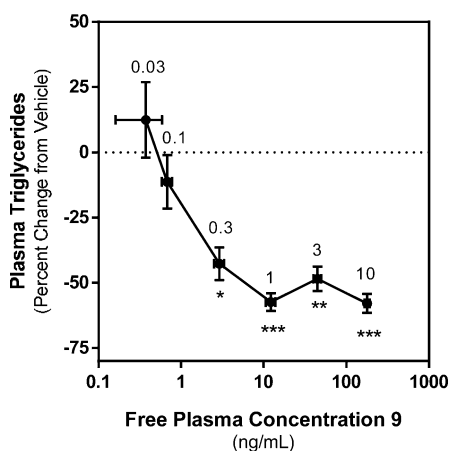


**Figure 3.** Acute effects of **9** on plasma triacylglycerol levels. Dose-dependent effects of **9** on plasma TG levels in sucrose-fed rats. Triglyceride (TG) levels were determined in blood drawn from the tail vein 2 h after oral administration of the indicated dose of **9** or vehicle (0.5% methylcellulose,  $n = 8$  per group). TG levels in untreated animals were  $77.4 \pm 6.9$  mg/dL. Relationship between plasma free drug levels and the pharmacodynamic effect (TG lowering). Data are expressed as percent change from the vehicle-treated group and were analyzed using one-way ANOVA followed by Dunnett's multiple comparison test. \* $p < 0.05$ , \*\* $p < 0.001$ , \*\*\* $p < 0.0001$  compared to vehicle-treated animals. The values shown adjacent to the individual data points indicate the dose group (mg/kg). Plasma concentrations of **9** that were below the lower limit of quantification using LC-MS/MS were eliminated from the analysis.

inhibited by **9** (Figure 4A). Nonsignificant decreases in circulating lipids were also observed following treatment of chow-fed animals with **9** (Figure 4A,B). To characterize the effects of **9** on lipoprotein distribution, plasma samples from HFHC-fed mice were subjected to fast protein liquid chromatography (FPLC) fractionation. As previously described,<sup>30</sup> the vast majority (>90%) of circulating cholesterol was carried in the VLDL and intermediate-density lipoprotein (IDL)/LDL fractions. Treatment with **9** for 3 days resulted in a dramatic decrease in VLDL-associated cholesterol. Decreases in IDL/LDL cholesterol were also apparent (Figure 4C). Because blockade of hepatic VLDL secretion has been associated with hepatic lipid accumulation,<sup>31</sup> hepatic lipid content was assayed. Treatment with **9** in HFHC-fed *Ldlr*<sup>-/-</sup> mice resulted in a significant decrease (32%,  $p < 0.05$ ) in hepatic TG content.

Having demonstrated favorable in vivo efficacy in both acute and subchronic settings, compound **9** was also profiled in a panel of standard advanced in vitro safety assays. Compound **9** did not show significant hERG (human ether-a-go-go related gene) inhibition (patch clamp  $IC_{50} = 95 \mu\text{M}$ ; >300-fold selectivity over DGAT2  $IC_{50}$ ). Little or no reversible inhibition of major cytochrome P450s (CYP2B6, 2C8, 2C19, 2D6, 3A4/5) was observed up to  $30 \mu\text{M}$  ( $IC_{50}$ s >  $30 \mu\text{M}$ ), indicating a low drug–drug interaction risk from reversible inhibition of these CYPs. No genetic toxicology risks were identified, with negative findings in an Ames mutagenicity assay and an in vitro micronucleus assay in TK6 cells, both in the presence and absence of the metabolic activation. On the basis of its favorable overall profile, compound **9** (PF-06424439)<sup>32</sup> was selected as a preclinical candidate for evaluation in regulatory toxicology studies.

## CONCLUSION

In summary, the first class of small-molecule DGAT2 inhibitors suitable for in vivo testing has been identified by optimization of a hit from high-throughput screening. The first round of optimization afforded a potent DGAT2 inhibitor such as **5** with significant improvement in LipE. The strategic introduction of an  $sp^3$ -carbon spacer to simultaneously improve both *N*-glucuronidation and off-target selectivity was a key design element leading to the discovery of the preclinical candidate **9** (PF-06424439). To our knowledge, PF-06424439 was the first orally bioavailable small-molecule DGAT2 inhibitor evaluated in vivo, demonstrating favorable effects on hepatic and circulating lipid levels in rats.<sup>15</sup> More detailed in vitro and in vivo pharmacological characterization of PF-06424439 will be described in future publications.

## EXPERIMENTAL SECTION

**General Experimental Methods.** All chemicals, reagents, and solvents were purchased from commercial sources and used without further purification unless otherwise noted. <sup>1</sup>H NMR data are reported relative to residual solvent signals and are reported as follows: chemical shift ( $\delta$  ppm), multiplicity, coupling constant (Hz), and integration. The multiplicities are denoted as follows: s, singlet; d, doublet; t, triplet; q, quartet; sept, septet; m, multiplet; br s, broad singlet; app, apparent. Silica gel chromatography was performed using a medium pressure Biotage or ISCO system and columns prepackaged by various commercial vendors including Biotage and ISCO. Whatman precoated silica gel plates (250  $\mu\text{m}$ ) were used for analytical thin-layer chromatography (TLC). The terms “concentrated” and “evaporated” refer to the removal of solvent at reduced pressure on a rotary evaporator with a water bath temperature not exceeding 60 °C. Purity of final compounds was assessed by reversed-phase HPLC with UV detection at 215 nm; all tested compounds were >95% purity unless otherwise noted. **Safety note:** Sodium hydride and DMSO can react explosively, please take appropriate precautions in using this reagent/solvent combination.

(*R*)-1-(2-(2-Cyclopropylpyrimidin-4-yl)-3*H*-imidazo[4,5-*b*]pyridin-5-yl)piperidin-3-yl(pyrrolidin-1-yl)methanone (**5**). Step 1: (*R*)-*tert*-Butyl 3-(pyrrolidine-1-carbonyl)piperidine-1-carboxylate. To a solution of (*R*)-1-(*tert*-butoxycarbonyl)piperidine-3-carboxylic acid (50.6 g, 221 mmol, 1 equiv) in anhydrous tetrahydrofuran (552 mL) at 2 °C was added 1,1'-carbonyldiimidazole (77.6 g, 460 mmol, 2.1 equiv). The mixture was stirred at room temperature for 2 h then cooled to 10 °C, whereupon pyrrolidine (74.0 mL, 890 mmol, 4.0 equiv) was added slowly. The reaction mixture was stirred at room temperature for 18 h. The solvent was removed under reduced pressure, and water (200 mL) was added to the residue. The mixture was extracted with ethyl acetate (2×). The combined organics were washed sequentially with 1*N* aqueous hydrochloric acid (4 × 200 mL) and with a saturated aqueous solution of sodium bicarbonate (2 × 200 mL). The organics were dried over magnesium sulfate, filtered, and concentrated under reduced pressure to afford (*R*)-*tert*-butyl 3-(pyrrolidine-1-carbonyl)piperidine-1-carboxylate as a white solid (58.8 g, 94%). The compound was used in the next step without further purification. <sup>1</sup>H NMR (400 MHz, CD<sub>3</sub>OD)  $\delta$  1.38–1.57 (m, 10H), 1.59–1.67 (m, 1H), 1.69–1.77 (m, 1H), 1.80–2.05 (m, 5H), 2.52–2.62 (m, 1H), 2.67–2.94 (m, 2H), 3.33–3.46 (m, 2H), 3.51–3.66 (m, 2H), 3.98–4.12 (m, 2H). MS ( $M + H$ )<sup>+</sup> = 283.3.

Step 2: (*R*)-Piperidin-3-yl(pyrrolidin-1-yl)methanone hydrochloride. To a solution of (*R*)-*tert*-butyl 3-(pyrrolidine-1-carbonyl)piperidine-1-carboxylate (58.8 g, 208 mmol, 1 equiv) in anhydrous dichloromethane (100 mL) was added hydrogen chloride in 1,4-dioxane (4*M*, 260 mL, 1040 mmol, 5.0 equiv). The reaction mixture was stirred vigorously at room temperature for 1 h. The solvent was removed under reduced pressure, and the residue was left standing overnight at room temperature. The residue was triturated with diethyl ether (250 mL). The diethyl ether was decanted and dichloromethane was added, followed by sonication in a warm water bath. The solvent

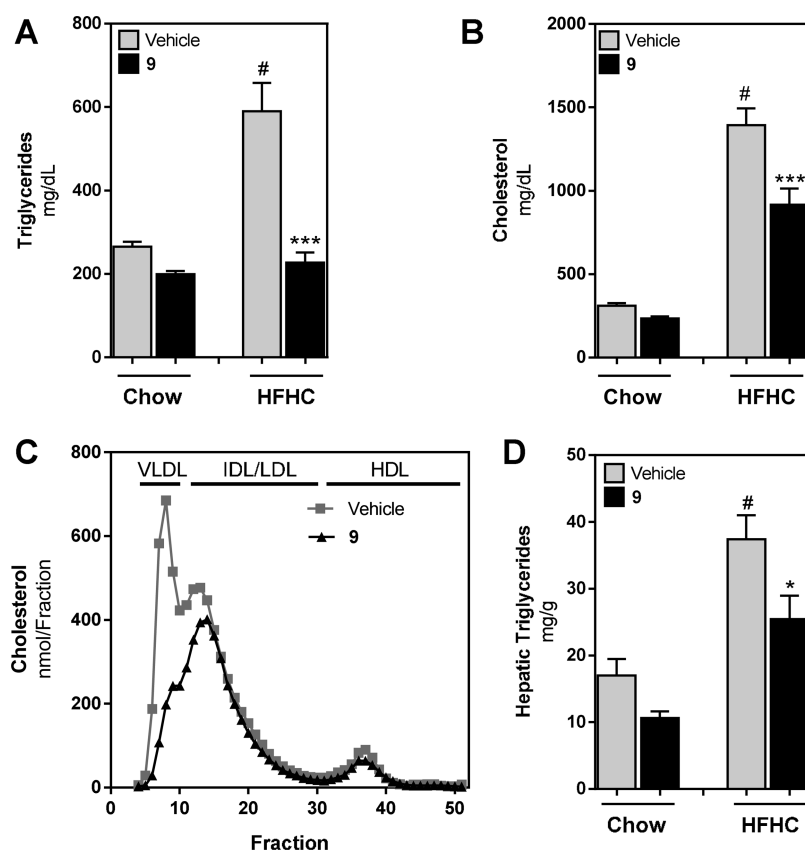


**Figure 4.** Effects of **9** on plasma and hepatic lipids in LDLr knockout mice (*Ldlr*<sup>-/-</sup>). Male *Ldlr*<sup>-/-</sup> mice were maintained on regular chow or high-fat, high-cholesterol diet (HFHC) for 2 weeks prior to treatment with either 60 mg/kg/day (30 mg/kg BID) **9** or vehicle (0.5% w/v methylcellulose) for 3 days. (A) Plasma TG. (B) Total plasma cholesterol. (C) Plasma lipoprotein profiles were generated on plasma from HFHC diet-fed mice as described in the Experimental Section. Lipid values were corrected for recoveries of total plasma lipid from combined fractions. VLDL, IDL/LDL, and high-density lipoprotein (HDL) are defined as fractions 4–11, 12–30, and 31–52, respectively. (D) Hepatic TG content. Data are mean  $\pm$  SEM from 6–8 animals and were analyzed using one-way ANOVA followed by Tukey's multiple comparison test.

was removed under reduced pressure, and the resulting solid was placed under high vacuum at 40 °C for 1 h to afford (*R*)-piperidin-3-yl(pyrrrolidin-1-yl)methanone hydrochloride (48.41 g, >100%). The material was used in the next step without further purification. <sup>1</sup>H NMR (400 MHz, CD<sub>3</sub>OD)  $\delta$  1.75–2.05 (m, 8H), 3.04–3.17 (m, 2H), 3.19–3.28 (m, 3H), 3.35–3.66 (m, 4H). MS (*M* + *H*)<sup>+</sup> = 183.3.

Step 3: (*R*)-(1-(6-Amino-5-nitropyridin-2-yl)piperidin-3-yl)(pyrrrolidin-1-yl)methanone. To a suspension of (*R*)-piperidin-3-yl(pyrrrolidin-1-yl)methanone hydrochloride (208 mmol, 1.1 equiv) from step 2 in anhydrous acetonitrile (200 mL) at 10 °C was added triethylamine (50.0 mL, 358 mmol, 1.9 equiv). The suspension was poured into a 2 L three-neck flask equipped with a thermometer and a magnetic stirrer. The original flask was rinsed with anhydrous acetonitrile and triethylamine (80.0 mL, 573 mmol, 3.0 equiv), with sonication. The suspensions were combined and cooled to 10 °C, and 6-chloro-3-nitropyridin-2-amine (32.9 g, 190 mmol, 1 equiv) was added. The bright-yellow solution was stirred under nitrogen, while the temperature was increased gradually to 80 °C over 1 h. The reaction mixture was then cooled to room temperature. The resulting suspension was filtered, and the solids were rinsed with ethyl acetate. The filtrate was concentrated under reduced pressure. A saturated aqueous solution of ammonium chloride (500 mL) was added to the residue, and the mixture was extracted into ethyl acetate (2 $\times$ ). The combined organics were washed with brine, dried over magnesium sulfate, filtered, and concentrated under reduced pressure, and the resulting residue was dried for 18 h under high vacuum to afford (*R*)-(1-(6-amino-5-nitropyridin-2-yl)piperidin-3-yl)(pyrrrolidin-1-yl)methanone as a yellow foam (63.5 g, > 100%), which was used without further purification. <sup>1</sup>H NMR (400 MHz, CD<sub>3</sub>OD)  $\delta$  1.47–1.64 (m, 1H), 1.71–2.07 (m, 7H), 2.50–2.70 (m, 1H), 2.98–3.04 (m, 2H),

3.33–3.46 (m, 2H), 3.45–3.55 (m, 1H), 3.60–3.70 (m, 1H), 4.41 (br s, 1H), 4.68 (br s, 1H), 6.23 (d, *J* = 9.6 Hz, 1H), 8.05 (d, *J* = 9.6 Hz, 1H). MS (*M* + *H*)<sup>+</sup> = 320.4.

Step 4: (*R*)-(1-(5,6-Diaminopyridin-2-yl)piperidin-3-yl)(pyrrrolidin-1-yl)methanone dihydrochloride. Into a Parr bottle was added 10% palladium-on-carbon (50% wet, 1.49 g) followed by ethanol (10 mL) which was previously bubbled with nitrogen and cooled to 0 °C. (*R*)-(1-(6-Amino-5-nitropyridin-2-yl)piperidin-3-yl)(pyrrrolidin-1-yl)methanone (10.6 g, 33.2 mmol, 1 equiv) in ethanol (84 mL), and a solution of concentrated hydrochloric acid (8.59 mL, 99.6 mmol, 3.0 equiv) in ethanol (10 mL) was added to the Parr bottle under a nitrogen atmosphere. The reaction mixture was purged with nitrogen and evacuated (3 $\times$ ). The mixture was submitted to a hydrogen atmosphere (45 psi). A drop in pressure was observed, and hydrogen pressure was increased to 46 psi. This process was repeated several times over a period of 30 min. The mixture was shaken for a total of 1 h and filtered through Celite rinsing with ethanol (0.7 L) and methanol (1.5 L). The filtrate was concentrated, and the resulting solid was dried under high vacuum to afford the title compound (12.0 g, 99%). The material was used without further purification. <sup>1</sup>H NMR (400 MHz, CD<sub>3</sub>OD)  $\delta$  1.71–1.81 (m, 2H), 1.88–1.95 (m, 3H), 1.98–2.12 (m, 3H), 2.89–2.95 (m, 1H), 3.38–3.55 (m, 5H), 3.66–3.72 (m, 1H), 3.97 (d, *J* = 12.7 Hz, 1H), 3.98 (dd, *J* = 13.7, 3.7 Hz, 1H), 6.39 (d, *J* = 9.3 Hz, 1H), 7.63 (d, *J* = 9.0 Hz, 1H). MS (*M* + *H*)<sup>+</sup> = 290.2.

Step 5: 2-Cyclopropylpyrimidine-4-carbonitrile. To a solution of 2-cyclopropylpyrimidine-4-carbaldehyde (29.1 g, 197 mmol, 1.0 equiv) in *N,N*-dimethylformamide (200 mL) was added hydroxylamine hydrochloride (13.9 g, 197 mmol, 1 equiv) and a solution of triethylamine (35.0 mL, 250 mmol, 1.3 equiv) in *N,N*-dimethylformamide (40 mL) at room temperature. A 50% solution of 1-

propanephosphonic anhydride in *N,N*-dimethylformamide (140 mL, 230 mmol, 1.2 equiv) was added, and the reaction mixture was stirred at 110 °C for 18 h. The mixture was cooled to room temperature, and a saturated aqueous solution of sodium bicarbonate and ethyl acetate was added. The mixture was stirred vigorously, and solid sodium bicarbonate was added. The mixture was filtered to remove undissolved solids, and the layers were separated. The aqueous layer was extracted with ethyl acetate (3×). The combined organics were washed with water and brine, dried over sodium sulfate, filtered, and concentrated under reduced pressure, and the resulting residue was dried under high vacuum to afford 2-cyclopropylpyrimidine-4-carbonitrile (21.0 g, 73%). The material was used without further purification. <sup>1</sup>H NMR (400 MHz, CDCl<sub>3</sub>) δ 1.15–1.22 (m, 4H), 2.28–2.35 (m, 1H), 7.36 (d, *J* = 4.8 Hz, 1H), 8.76 (d, *J* = 4.8 Hz, 1H).

Step 6: Ethyl 2-cyclopropylpyrimidine-4-carbimidate. To a solution of 2-cyclopropylpyrimidine-4-carbonitrile (20.97 g, 144.5 mmol, 1 equiv) in ethanol (100 mL) was added a solution of sodium ethoxide (prepared from sodium metal (1.8 g, 78.9 mmol) in 30 mL of ethanol, 0.55 equiv). The reaction mixture was stirred at room temperature for 30 min. Diethyl ether (300 mL) and a saturated aqueous solution of ammonium chloride (50 mL) were added sequentially. The mixture was extracted with diethyl ether (3 × 100 mL). The combined organics were washed with brine (2 × 50 mL), dried over magnesium sulfate, filtered, and concentrated under reduced pressure, and the resulting residue was dried under high vacuum. The material was used without further purification. <sup>1</sup>H NMR (500 MHz, CDCl<sub>3</sub>) δ 1.06–1.13 (m, 2H), 1.16–1.22 (m, 2H), 1.41 (t, *J* = 7.1 Hz, 3H), 2.27–2.35 (m, 1H), 4.40 (q, *J* = 7.2 Hz, 2H), 7.48 (d, *J* = 5.1 Hz, 1H), 8.72 (d, *J* = 4.9 Hz, 1H) 9.26 (br s, 1H).

Step 7: (*R*)-(1-(2-(2-Cyclopropylpyrimidin-4-yl)-3H-imidazo[4,5-*b*]pyridin-5-yl)piperidin-3-yl)(pyrrolidin-1-yl)methanone (**5**). To a suspension of (*R*)-(1-(5,6-diaminopyridin-2-yl)piperidin-3-yl)(pyrrolidin-1-yl)methanone dihydrochloride (1.0 g, 2.8 mmol, 1.0 equiv) and acetic acid (2.5 mL, 43 mmol, 15 equiv) in ethanol (7 mL) was added triethylamine (1.5 mL, 10.8 mmol, 3.9 equiv) and a solution of ethyl 2-cyclopropylpyrimidine-4-carbimidate (530 mg, 2.8 mmol, 1 equiv) in ethanol (3 mL). The reaction mixture was heated under reflux for 1 h and cooled to room temperature. The solvent was removed under reduced pressure, and ethyl acetate (100 mL) was added to the residue followed by water (10 mL) and a saturated aqueous solution of ammonium chloride (50 mL). The layers were separated, and the organics were washed sequentially with a saturated aqueous solution of sodium bicarbonate (75 mL) and brine (50 mL), dried over magnesium sulfate, filtered, and concentrated under reduced pressure. To the resulting residue was added dichloromethane (4 mL) and methyl *tert*-butyl ether (35 mL). The mixture was stirred at 40 °C until it was homogeneous. The solution was cooled to room temperature and stirred for 18 h. The resulting solids were filtered and rinsed with ether to afford **5** (1.02 g, 62%). <sup>1</sup>H NMR (400 MHz, CDCl<sub>3</sub>) δ 1.10–1.17 (m, 2H), 1.18–1.23 (m, 2H), 1.57–1.70 (m, 1H), 1.82–2.05 (m, 7H), 2.27–2.34 (m, 1H), 2.63–2.72 (m, 1H), 2.97–3.07 (m, 1H), 3.14–3.22 (m, 1H), 3.43–3.54 (m, 3H), 3.58–3.67 (m, 1H), 4.37 (d, *J* = 13.7 Hz, 1H), 4.53 (d, *J* = 12.9 Hz, 1H), 6.76 (d, *J* = 9.0 Hz, 1H), 7.82–7.90 (m, 2H), 8.67 (d, *J* = 5.3 Hz, 1H), 10.27 (br s, 1H). MS (*M* + *H*)<sup>+</sup> = 418.5.

(*R*)-(1-(2-(1-(4-Chloro-1H-pyrazol-1-yl)cyclopropyl)-3H-imidazo[4,5-*b*]pyridin-5-yl)piperidin-3-yl)(pyrrolidin-1-yl)methanone (**9**). Step 1: 1-(4-Chloro-1H-pyrazol-1-yl)cyclopropanecarbonitrile. **Safety note:** Sodium hydride and DMSO can react explosively, please take appropriate precautions in using this reagent/solvent combination. Into a four-neck, 2 L round-bottom flask, previously dried with a heat gun under high vacuum, was added DMSO (175 mL). The flask was placed in a 10 °C bath, and sodium hydride (60% oil dispersion, 17.0 g, 300 mmol, 4.2 equiv) was added portionwise with stirring under nitrogen. The resulting suspension was stirred for 10 min before a solution of 2-(4-chloro-1H-pyrazol-1-yl)acetonitrile (10.0 g, 70.6 mmol, 1 equiv) and 1,2-dibromoethane (18.3 mL, 213 mmol, 3.0 equiv) in DMSO (175 mL) was added dropwise over a period of 30 min. The internal temperature was kept between 13 and 20 °C during the addition process. The reaction mixture was stirred for 5.5 h while

keeping the internal temperature at or below 20 °C, followed by stirring for an additional 1 h at room temperature. The mixture was cooled to 10 °C, and then a saturated aqueous solution of ammonium chloride (600 mL) was slowly added. The mixture was stirred at 10 °C for 15 min and extracted with ethyl acetate (3 × 1 L). The combined organics were washed with brine, dried over sodium sulfate, filtered, and concentrated under reduced pressure. The crude material was purified via flash chromatography (10–100% dichloromethane in hexanes), and the resulting residue was crystallized from a mixture of hexanes/diethyl ether to afford 1-(4-chloro-1H-pyrazol-1-yl)cyclopropanecarbonitrile (7.65 g, 65%). <sup>1</sup>H NMR (400 MHz, CDCl<sub>3</sub>) δ 1.77–1.82 (m, 4H), 7.45 (s, 1H), 7.60 (s, 1H). MS (*M*)<sup>+</sup> = 167.

Step 2: Ethyl 1-(4-chloro-1H-pyrazol-1-yl)cyclopropanecarbimidate. To a solution of 1-(4-chloro-1H-pyrazol-1-yl)cyclopropanecarbonitrile (17.3 g, 103 mmol, 1 equiv) in ethanol (50 mL) was added sodium ethoxide (prepared from sodium metal (3.2 g, 139 mmol) in 150 mL of ethanol, 1.3 equiv). The reaction mixture was stirred at 70 °C for 2 h to afford ethyl 1-(4-chloro-1H-pyrazol-1-yl)cyclopropanecarbimidate, which was used for the next step without further purification. An aliquot of the solution was concentrated for analysis. <sup>1</sup>H NMR (400 MHz, CDCl<sub>3</sub>): δ 1.24 (t, *J* = 7.24 Hz, 3H, obscured by residual ethanol), 1.42–1.48 (m, 2H), 1.69–1.74 (m, 2H), 4.15 (q, *J* = 7.0 Hz, 2H), 7.50 (s, 1H), 7.51 (s, 1H).

Step 3: (*R*)-(1-(2-(1-(4-Chloro-1H-pyrazol-1-yl)cyclopropyl)-3H-imidazo[4,5-*b*]pyridin-5-yl)piperidin-3-yl)(pyrrolidin-1-yl)methanone (**9**). To a solution of (*R*)-(1-(5,6-diaminopyridin-2-yl)piperidin-3-yl)(pyrrolidin-1-yl)methanone dihydrochloride (5.50 g, 15.2 mmol, 1 equiv) and acetic acid (17.4 mL, 305 mmol, 20 equiv) in ethanol (20 mL) was added a solution of ethyl 1-(4-chloro-1H-pyrazol-1-yl)cyclopropanecarbimidate (3.25 g, 15.2 mmol, 1.0 equiv) in ethanol (30 mL) followed by triethylamine (12.7 mL, 91.2 mmol, 6.0 equiv). The resulting mixture was purged with nitrogen. The reaction mixture was stirred at 100 °C for 18 h. The mixture was cooled to room temperature, and the solvent was removed under reduced pressure. The residue was partitioned between a saturated aqueous solution of ammonium chloride (50 mL) and dichloromethane (50 mL). The aqueous layer was extracted with dichloromethane (50 mL). The combined organics were washed with a saturated aqueous solution of sodium bicarbonate, and the resulting aqueous layer was extracted with dichloromethane (50 mL). The organics were combined, washed with brine, dried over sodium sulfate, filtered, and concentrated under reduced pressure. The crude material was purified via flash chromatography (0–5% methanol in dichloromethane) to afford **9** (6.33 g, 94%). <sup>1</sup>H NMR (500 MHz, CDCl<sub>3</sub>) δ 1.55–1.70 (m, 1H), 1.72–2.05 (m, 11H), 2.60–2.70 (m, 1H), 2.90–2.95 (m, 1H), 3.03–3.10 (m, 1H), 3.42–3.50 (m, 3H), 3.56–3.62 (m, 1H), 4.20–4.25 (m, 1H), 4.38–4.44 (m, 1H), 6.62–6.68 (m, 1H), 7.59 (s, 1H), 7.63 (s, 1H), 7.66–7.72 (m, 1H). MS (*M* + *H*)<sup>+</sup> = 440.

(*R*)-(1-(2-(1-(4-Chloro-1H-pyrazol-1-yl)cyclopropyl)-3H-imidazo[4,5-*b*]pyridin-5-yl)piperidin-3-yl)(pyrrolidin-1-yl)methanone Methanesulfonate (**9-*MsOH***). To a solution of **9** (56.5 g, 128 mmol, 1 equiv) in acetonitrile (130 mL) was added methanesulfonic acid (8.33 mL, 128 mmol, 1.0 equiv). The mixture was stirred at room temperature for 18 h. The mixture was filtered, and the solids were rinsed with acetonitrile. The solids were collected and dried under high vacuum for 1 h to afford **9-*MsOH*** (62.5 g, 90%). <sup>1</sup>H NMR (400 MHz, CDCl<sub>3</sub>) δ 1.65–1.75 (m, 1H), 1.84–2.13 (m, 11H), 2.75–2.85 (m, 1H), 2.87 (s, 3H), 3.28–3.35 (m, 1H), 3.39–3.57 (m, 4H), 3.65–3.72 (m, 1H), 4.02–4.09 (m, 1H), 4.11–4.17 (m, 1H), 6.73–6.82 (m, 1H), 7.55 (s, 1H), 7.76 (s, 1H), 8.13 (d, *J* = 9.0 Hz, 1H). MS (*M* + *H*)<sup>+</sup> = 440; mp = 212–214 °C. Anal. Calcd for C<sub>22</sub>H<sub>26</sub>ClN<sub>7</sub>O·CH<sub>4</sub>O<sub>3</sub>S: C, 51.53; H, 5.64; N, 18.29; Cl, 6.61; S, 5.98. Found: C, 51.28; H, 5.65; N, 18.19; Cl, 6.56; S, 5.96.

**DGAT2 Assay and Determination of IC<sub>50</sub> Values.** DGAT2 activity was determined by measuring the incorporation of the [1-<sup>14</sup>C]decanoyl moiety into triacylglycerol using [1-<sup>14</sup>C]decanoyl-CoA and 1,2-didecanoyl-*sn*-glycerol as substrates. The final assay mixture contained 50 mM Hepes-NaOH, pH 7.4, 6 μM [1-<sup>14</sup>C]-decanoyl-CoA (50 mCi/mmol, PerkinElmer, Waltham, MA), 25 μM

1,2-didecanoyl-*sn*-glycerol (Avanti Polar Lipids, Alabaster, AL), 10 mM MgCl<sub>2</sub>, 100 mM methyl arachidonyl fluorophosphonate (MAFP, Cayman Chemical, Ann Arbor, MI), 0.01% BSA (fatty acid free, Sigma-Aldrich, St. Louis, MO), 5% DMSO, 2.5% acetone, and 0.1 μg of the detergent-solubilized DGAT2 membrane. The reactions were carried out in 384-well white Polyplates (PerkinElmer) in a total volume of 20 μL. To 1 μL of compounds dissolved in 100% DMSO and spotted at the bottom of each well, 5 μL of 0.04% BSA was added and the mixture was kept at room temperature for 20 min. To this mixture, 10 μL of the detergent-solubilized DGAT2 membrane fraction (0.01 mg/mL) diluted in 100 mM Hepes–NaOH, pH 7.4, 20 mM MgCl<sub>2</sub> containing 200 nM MAFP (dried from ethyl acetate stock solution under argon gas and dissolved in DMSO as 5 mM stock) was added. After this mixture was preincubated at room temperature for 120 min, DGAT2 reactions were initiated by the addition of 4 μL of substrates containing 30 μM [1-<sup>14</sup>C]decanoyl-CoA and 125 μM 1,2-didecanoyl-*sn*-glycerol dissolved in 12.5% acetone. The reaction mixtures were incubated at room temperature for 40 min, and the reactions were stopped by addition of 5 μL of 1% H<sub>3</sub>PO<sub>4</sub>. After the addition of 45 μL of MicroScint-E (PerkinElmer), plates were sealed with Top Seal-A covers (PerkinElmer) and phase partitioning of substrates and products was achieved using a HT-91100 microplate orbital shaker (Big Bear Automation, Santa Clara, CA). Plates were centrifuged at 2000g for 1 min and then were sealed again with fresh covers before reading in a 1450 Microbeta Wallac Trilux scintillation counter (PerkinElmer). DGAT2 activity was measured by quantifying the generated product [<sup>14</sup>C]tridecanoylglycerol in the upper organic phase. Background activity obtained using 50 μM of (1*R*, 2*R*)-2-((3'-fluoro-4'-[(6-fluoro-1, 3-benzothiazol-2-yl)amino]-1,1'-biphenyl-4-yl)-carbonyl)cyclopentanecarboxylic acid (US 20040224997, example 26) for complete inhibition of DGAT2 was subtracted from all reactions. Inhibitors were tested at 11 different concentrations to generate IC<sub>50</sub> values for each compound. The 11 inhibitor concentrations employed typically included 50, 15.8, 5, 1.58, 0.50, 0.16, 0.05, 0.016, 0.005, 0.0016, and 0.0005 μM. The data were plotted as percentage of inhibition versus inhibitor concentration and fit to the equation,  $y = 100/[1 + (x/IC_{50})^z]$ , where IC<sub>50</sub> is the inhibitor concentration at 50% inhibition and  $z$  is the Hill slope (the slope of the curve at its inflection point).

**Determination of IC<sub>50</sub> Values for DGAT1 and MGAT1/2/3 Inhibition.** Enzyme activity for DGAT1 and MGAT3 was determined by measuring the incorporation of the [1-<sup>14</sup>C]decanoyl moiety into TG using [1-<sup>14</sup>C]decanoyl-CoA and 1,2-didecanoyl-*sn*-glycerol as substrates. Enzyme activity for MGAT1 was determined by measuring the incorporation of the [1-<sup>14</sup>C]decanoyl moiety into DAG using [1-<sup>14</sup>C]decanoyl-CoA and 2-oleoylglycerol as substrates. MGAT2 activity was determined by measuring the incorporation of the [1-<sup>14</sup>C]decanoyl moiety into DAG using [1-<sup>14</sup>C]decanoyl-CoA and 1-decanoyl-*rac*-glycerol as substrates. All assays were performed in 384-well Polyplates in a total volume of 20 μL. The final assay mixture contained 50 mM Hepes–NaOH, pH 7.4, 10 mM MgCl<sub>2</sub>, the indicated concentrations of substrates (below), 100 nM MAFP, 0.01% Triton X-100, 5% DMSO, 2.5% acetone, and the indicated amount of each enzyme. The final substrate concentrations in the assay were 7.5 μM [1-<sup>14</sup>C]decanoyl-CoA and 10 μM 1,2-didecanoyl-*sn*-glycerol for DGAT1, 2 μM [1-<sup>14</sup>C]decanoyl-CoA and 20 μM 2-oleoylglycerol (Sigma-Aldrich) for MGAT1, 4 μM [1-<sup>14</sup>C]decanoyl-CoA and 25 μM 1-decanoyl-*rac*-glycerol (Nu-Check Prep Inc., Elysian, MN) for MGAT2, 2 μM [1-<sup>14</sup>C]decanoyl-CoA and 35 μM 1,2-didecanoyl-*sn*-glycerol for MGAT3. All compounds were preincubated with each enzyme for 30 min before initiating reactions by addition of substrates. Typically, 1 μg of DGAT1 microsomal fraction was required for each reaction per well. MGAT1, MGAT2, and MGAT3 reactions required 0.12, 0.006, and 0.05 μg of the detergent-solubilized membrane fractions, respectively, for each reaction per well. Typical reaction times were 30–70 min at room temperature. The radioactive DAG and TG products generated were quantified by scintillation counting following reaction quenching and phase partitioning as described in the DGAT2 assay above. Background activity, typical dose response

range, and data analysis for IC<sub>50</sub> determinations were identical to those described in the DGAT2 assay.

**Determination of IC<sub>50</sub> Values for TG Synthesis in Fresh Human Hepatocytes.** Fresh human hepatocytes (Triangle Research Laboratories, Research Triangle Park, NC, Celsis IVT, Baltimore, MD, or Life Technologies, Grand Island, NY) (50000 cells per well) were seeded into collagen I coated 96-well plates (BD Biosciences, Woburn, MA) and maintained overnight in Williams' E media prior to determination of DGAT2 activity. Media was aspirated and the cells incubated with 400 μM sodium dodecanoate (Sigma-Aldrich, St. Louis, MO) in Williams' E media for 40 min prior to the addition of a selective DGAT1 inhibitor {*trans*-4-[4-(4-amino-5-oxo-7,8-dihydropyrimido[5,4-*f*][1,4]oxazepin-6(5*H*)-yl)phenyl]cyclohexyl}-acetic acid (PF-04620110, 3 μM) and eight concentrations of compound **9** ranging from 0.0003 to 1 μM. Both compounds were dissolved in dimethyl sulfoxide (DMSO), and the final concentration of DMSO in each well was kept constant at 0.25% volume/volume (v/v). After a further 20 min incubation, 5 μL of [<sup>14</sup>C]glycerol (American Radio Chemicals, St. Louis, MO) (0.2 μCi) was added to each well and mixed by gentle pipetting. The plate was returned to the incubator (37 °C, 5% carbon dioxide) for 3.5 h prior to aspiration of the media and addition of 100 μL of isopropyl alcohol:THF (9:1). The plate was shaken for 15 min, centrifuged at 3000 rpm for 5 min, and 50 μL of supernatant from each well applied to TLC lane (Whatman LK6D Silica Gel Plates). Radiolabeled lipids were resolved using a two-solvent system. Solvent 1 contained a 100:100:100:40:36 mixture of ethyl acetate:isopropyl alcohol:CHCl<sub>3</sub>:MeOH:0.25% KCl and solvent 2 a 70:27:3 hexane:diethyl ether:acetic acid mix. The TLC plate was dried under nitrogen for 30 min and [<sup>14</sup>C]-calibrators added to a vacant lane. Bands were visualized and quantitated using a Molecular Dynamics' Storm 860 PhosphorImager system following 18–36 h exposure to a PhosphorImager screen. The IC<sub>50</sub> was determined using GraphPad Prism (GraphPad Software, Inc., La Jolla, CA).

**Acute Effects of Compound **9** on Plasma Triacylglycerol Levels.** Male Sprague–Dawley rats (~200 g, Harlan Laboratories, Inc., Madison, WA) were fed a high-sucrose, low-fat diet (TD.03045, Harlan Laboratories, Inc.) 2 days prior to the study. On the day of the study, animals were fasted for 4 h prior to treatment. Immediately before dosing, blood was drawn from the lateral tail vein into a dipotassium ethylenediaminetetraacetic acid (K<sub>2</sub> EDTA)-containing tube (Microtainer, Becton Dickinson, Franklin Lakes, NJ). Following centrifugation, the plasma was transferred to a fresh tube for the determination of TG levels using a Roche Hitachi Chemistry analyzer (Roche Diagnostics Corporation, Indianapolis, IN). Animals were dosed with 0.01, 0.03, 0.1, 0.3, 1, 3, 10 mg/kg po compound **9** as a solution in 0.5% w/v methylcellulose (10 mL/kg dosing volume). Vehicle-treated animals received 0.5% methylcellulose alone. After a further 2 h, blood was drawn and TG determined as described above. Data were expressed as percent change from vehicle-treated animals. The level of **9** was determined in these plasma samples using LC-MS/MS.

**Effects of Compound **9** on Plasma and Hepatic Lipids in LDLr Knockout Mice (*Ldlr*<sup>-/-</sup>).** Male low-density lipoprotein receptor (LDLR) knockout mice (B6.129S7-*Ldlr*<sup>tm1Her</sup>/*J*) were obtained from The Jackson Laboratory (Bar Harbor, Maine) at 7–8 weeks of age and maintained on either standard laboratory chow (PicoLab Rodent Diet 20 no. 5053, LabDiet, St. Louis, MO) or a high-fat, high-cholesterol diet (HFHC, D12108, Research Diets Inc., New Brunswick, NJ) which contains ~40 kcal% from fat and 1.25% w/w cholesterol for 2 weeks prior to treatment. Animals were dosed with either 60 mg/kg/day (30 mg/kg BID) of **9** or vehicle (0.5% w/v methylcellulose) for 3 days (total of five doses). On the final day, food was withdrawn at 06:00, and the animals were dosed at 10:00 and sacrificed 2 h later. All animals were sacrificed by carbon dioxide asphyxiation, and blood for lipoprotein analysis was collected by cardiac puncture. Livers were excised, immediately frozen in liquid nitrogen, and held at –80 °C until analysis. Plasma TG and cholesterol were determined as described above. Plasma lipoproteins were separated by FPLC essentially as described elsewhere.<sup>33</sup> Briefly, 200 μL aliquots of plasma pooled from eight mice were injected inline to

two Superose 6 columns (GE Healthcare Biosciences, Pittsburgh, PA) connected in tandem at a flow rate of 0.2 mL/min and fractions were collected. Cholesterol was determined by standard enzymatic assay. Lipid values, nmol/fraction, were corrected for recoveries of total plasma cholesterol from combined fractions. Total lipids were extracted from the livers using the Folch method.<sup>34</sup> All extraction solvents contained 50  $\mu$ M butylated hydroxytoluene as antioxidant. Neutral lipids were isolated from the total lipid extracts using aminopropyl solid phase extraction columns as previously described.<sup>35</sup> The neutral lipid fraction was in turn dried down under nitrogen and resuspended in isoctane:isopropyl alcohol (98:2). Neutral lipids were separated and detected using normal phase cyanopropyl high-performance liquid chromatography (HPLC) and a charged aerosol detector.<sup>36</sup> Data are expressed as mg/g wet weight of liver.

## ■ ASSOCIATED CONTENT

### ● Supporting Information

The Supporting Information is available free of charge on the ACS Publications website at DOI: 10.1021/acs.jmedchem.5b01006.

Procedures for the synthesis of compounds 1–4 and 6–8; generation of constructs for DGAT1/2 and MGAT1/2/3; expression and preparation of membrane and microsomal fractions; selectivity data of compound 5 (PDF)

Molecular formula strings (CSV)

## ■ AUTHOR INFORMATION

### Corresponding Authors

\*For K.F.: E-mail, [Kentaro.Futatsugi@pfizer.com](mailto:Kentaro.Futatsugi@pfizer.com).

\*For D.W.K.: E-mail, [Daniel.W.Kung@pfizer.com](mailto:Daniel.W.Kung@pfizer.com).

### Notes

The authors declare the following competing financial interest(s): All authors were employed by Pfizer Inc at the time this work was done.

## ■ ACKNOWLEDGMENTS

We thank David Bernhardson, Peter Dorff, and Matthew F. Sammons for their contributions to synthesis, Jared Milbank and Jian Wang for their contributions to data analytics and computational chemistry, Steven Hawrylik, Tracy B. Phillips, Tim Subashi, and George Tkalcovic for expression of DGAT1/2, MGAT1/2/3 enzymes, and Alfin Vaz for metabolite identification works.

## ■ ABBREVIATIONS USED

DGAT2, diacylglycerol acyltransferase 2; LDL, low-density lipoprotein; LDLr, low-density lipoprotein receptor; MGAT1, monoacylglycerol acyltransferase 1; MGAT2, monoacylglycerol acyltransferase 2; MGAT3, monoacylglycerol acyltransferase 3; DGAT1, diacylglycerol acyltransferase 1; TG, triacylglycerol; MAG, monoacylglycerol; DAG, diacylglycerol; TC, total cholesterol; NASH, nonalcoholic steatohepatitis; NAFLD, nonalcoholic fatty liver disease; MAFP, methyl arachidonyl fluorophosphonate; LipE, lipophilic efficiency; HLM, human liver microsome; CYP, cytochrome P450; Papp, apparent passive permeability; SAR, structure–activity relationship; MW, molecular weight; RRCK, Ralph Russ canine kidney cells; UGT, UDP-glucuronosyltransferase; 1H-benzotriazol-1-yloxytris(dimethylamino)phosphonium hexafluorophosphate; T<sub>3</sub>P, 1-propanephosphonic anhydride; NMM, N-methyl morpholine; MsOH, methanesulfonic acid;  $f_{u,p}$ , fraction unbound in plasma

## ■ REFERENCES

- (1) Raised cholesterol: Situation and Trends. *Global Health Observatory (GHO) Data*; World Health Organization: Geneva, 2015; [http://www.who.int/gho/ncd/risk\\_factors/cholesterol\\_text/en/](http://www.who.int/gho/ncd/risk_factors/cholesterol_text/en/).
- (2) Baigent, C.; Keech, A.; Kearney, P. M.; Blackwell, L.; Buck, G.; Pollicino, C.; Kirby, A.; Sourjina, T.; Peto, R.; Collins, R.; Simes, R.; Cholesterol Treatment Trialists' (CTT) Collaborators. Efficacy and safety of cholesterol-lowering treatment: prospective meta-analysis of data from 90,056 participants in 14 randomised trials of statins. *Lancet* **2005**, *366* (9493), 1267–1278.
- (3) (a) Ridker, P. M.; Genest, J.; Boekholdt, S. M.; Libby, P.; Gotto, A. M.; Nordestgaard, B. G.; Mora, S.; MacFadyen, J. G.; Glynn, R. J.; Kastelein, J. J.; JUPITER Trial Study Group. HDL cholesterol and residual risk of first cardiovascular events after treatment with potent statin therapy: an analysis from the JUPITER trial. *Lancet* **2010**, (9738), 333–339. (b) Sampson, U. K.; Fazio, S.; Linton, M. F. Residual cardiovascular risk despite optimal LDL cholesterol reduction with statins: the evidence, etiology, and therapeutic challenges. *Curr. Atheroscler. Rep.* **2012**, *14* (1), 1–10.
- (4) (a) Do, R.; Willer, C. J.; Schmidt, E. M.; Sengupta, S.; Gao, C.; Peloso, G. M.; Gustafsson, S.; Kanoni, S.; Ganna, A.; Chen, J.; Buchkovich, M. L.; Mora, S.; Beckmann, J. S.; Bragg-Gresham, J. L.; Chang, H. Y.; Demirkan, A.; Den Hertog, H. M.; Donnelly, L. A.; Ehret, G. B.; Esko, T.; Feitosa, M. F.; Ferreira, T.; Fischer, K.; Fontanillas, P.; Fraser, R. M.; Freitag, D. F.; Gurdasani, D.; Heikkilä, K.; Hyppönen, E.; Isaacs, A.; Jackson, A. U.; Johansson, A.; Johnson, T.; Kaakinen, M.; Kettunen, J.; Kleber, M. E.; Li, X.; Luan, J.; Lyttikainen, L. P.; Magnusson, P. K.; Mangino, M.; Mihailov, E.; Montasser, M. E.; Muller-Nurasyid, M.; Nolte, I. M.; O'Connell, J. R.; Palmer, C. D.; Perola, M.; Petersen, A. K.; Sanna, S.; Saxena, R.; Service, S. K.; Shah, S.; Shungin, D.; Sidore, C.; Song, C.; Strawbridge, R. J.; Surakka, I.; Tanaka, T.; Teslovich, T. M.; Thorleifsson, G.; Van den Herik, E. G.; Voight, B. F.; Volcik, K. A.; Waite, L. L.; Wong, A.; Wu, Y.; Zhang, W.; Absher, D.; Asiki, G.; Barroso, I.; Been, L. F.; Bolton, J. L.; Bonnycastle, L. L.; Brambilla, P.; Burnett, M. S.; Cesana, G.; Dimitriou, M.; Doney, A. S.; Doring, A.; Elliott, P.; Epstein, S. E.; Eyjolfsson, G. I.; Gigante, B.; Goodarzi, M. O.; Grallert, H.; Gravitto, M. L.; Groves, C. J.; Hallmans, G.; Hartikainen, A. L.; Hayward, C.; Hernandez, D.; Hicks, A. A.; Holm, H.; Hung, Y. J.; Illig, T.; Jones, M. R.; Kaleebu, P.; Kastelein, J. J.; Khaw, K. T.; Kim, E.; Klopp, N.; Komulainen, P.; Kumari, M.; Langenberg, C.; Lehtimäki, T.; Lin, S. Y.; Lindstrom, J.; Loos, R. J.; Mach, F.; McArdle, W. L.; Meisinger, C.; Mitchell, B. D.; Muller, G.; Nagaraja, R.; Narisu, N.; Nieminen, T. V.; Nsubuga, R. N.; Olafsson, I.; Ong, K. K.; Palotie, A.; Papamarkou, T.; Pomilla, C.; Pouta, A.; Rader, D. J.; Reilly, M. P.; Ridker, P. M.; Rivadeneira, F.; Rudan, I.; Ruukonen, A.; Samani, N.; Scharnagl, H.; Seeley, J.; Silander, K.; Stancakova, A.; Stirrups, K.; Swift, A. J.; Tiret, L.; Uitterlinden, A. G.; van Pelt, L. J.; Vedantam, S.; Wainwright, N.; Wijmenga, C.; Wild, S. H.; Willemssen, G.; Wilsgaard, T.; Wilson, J. F.; Young, E. H.; Zhao, J. H.; Adair, L. S.; Arveiler, D.; Assimes, T. L.; Bandinelli, S.; Bennett, F.; Bochud, M.; Boehm, B. O.; Boomsma, D. I.; Borecki, I. B.; Bornstein, S. R.; Bovet, P.; Burnier, M.; Campbell, H.; Chakravarti, A.; Chambers, J. C.; Chen, Y. D.; Collins, F. S.; Cooper, R. S.; Danesh, J.; Dedoussis, G.; de Faire, U.; Feranil, A. B.; Ferrieres, J.; Ferrucci, L.; Freimer, N. B.; Gieger, C.; Groop, L. C.; Gudnason, V.; Gyllenstein, U.; Hamsten, A.; Harris, T. B.; Hingorani, A.; Hirschhorn, J. N.; Hofman, A.; Hovingh, G. K.; Hsiung, C. A.; Humphries, S. E.; Hunt, S. C.; Hveem, K.; Iribarren, C.; Jarvelin, M. R.; Julia, A.; Kahonen, M.; Kaprio, J.; Kesaniemi, A.; Kivimäki, M.; Kooner, J. S.; Koudstaal, P. J.; Krauss, R. M.; Kuh, D.; Kuusisto, J.; Kyvik, K. O.; Laakso, M.; Lakka, T. A.; Lind, L.; Lindgren, C. M.; Martin, N. G.; Marz, W.; McCarthy, M. I.; McKenzie, C. A.; Meneton, P.; Metspalu, A.; Moilanen, L.; Morris, A. D.; Munroe, P. B.; Njolstad, I.; Pedersen, N. L.; Power, C.; Pramstaller, P. P.; Price, J. F.; Psaty, B. M.; Quertermous, T.; Rauramaa, R.; Saleheen, D.; Salomaa, V.; Sanghera, D. K.; Saramies, J.; Schwarz, P. E.; Sheu, W. H.; Shuldiner, A. R.; Siegbahn, A.; Spector, T. D.; Stefansson, K.; Strachan, D. P.; Tayo, B. O.; Tremoli, E.; Tuomilehto, J.; Uusitupa, M.; van Duijn, C. M.;

- Vollenweider, P.; Wallentin, L.; Wareham, N. J.; Whitfield, J. B.; Wolffenduttel, B. H.; Altschuler, D.; Ordovas, J. M.; Boerwinkle, E.; Palmer, C. N.; Thorsteinsdottir, U.; Chasman, D. I.; Rotter, J. I.; Franks, P. W.; Ripatti, S.; Cupples, L. A.; Sandhu, M. S.; Rich, S. S.; Boehnke, M.; Deloukas, P.; Mohlke, K. L.; Ingelsson, E.; Abecasis, G. R.; Daly, M. J.; Neale, B. M.; Kathiresan, S. Common variants associated with plasma triglycerides and risk for coronary artery disease. *Nat. Genet.* **2013**, *45* (11), 1345–1352. (b) Goldberg, I. J.; Eckel, R. H.; McPherson, R. Triglycerides and heart disease: still a hypothesis? *Arterioscler., Thromb., Vasc. Biol.* **2011**, *31* (8), 1716–1725. (c) ACCORD Study Group; Ginsberg, H. N.; Elam, M. B.; Lovato, L. C.; Crouse, J. R., III; Leiter, L. A.; Linz, P.; Friedewald, W. T.; Buse, J. B.; Gerstein, H. C.; Probstfeld, J.; Grimm, R. H.; Ismail-Beigi, F.; Bigger, J. T.; Goff, D. C., Jr.; Cushman, W. C.; Simons-Morton, D. G.; Byington, R. P. Effects of combination lipid therapy in type 2 diabetes mellitus. *N. Engl. J. Med.* **2010**, *362* (17), 1563–1574. (d) Jorgensen, A. B.; Frikke-Schmidt, R.; Nordestgaard, B. G.; Tybjaerg-Hansen, A. Loss-of-function mutations in APOC3 and risk of ischemic vascular disease. *N. Engl. J. Med.* **2014**, *371* (1), 32–41. (e) The TG and HDL Working Group of the Exome Sequencing Project, National Heart, Lung, and Blood Institute; Crosby, J.; Peloso, G. M.; Auer, P. L.; Crosslin, D. R.; Stitzel, N. O.; Lange, L. A.; Lu, Y.; Tang, Z. Z.; Zhang, H.; Hindy, G.; Masca, N.; Stirrups, K.; Kanoni, S.; Do, R.; Jun, G.; Hu, Y.; Kang, H. M.; Xue, C.; Goel, A.; Farrall, M.; Duga, S.; Merlini, P. A.; Asselta, R.; Girelli, D.; Olivieri, O.; Martinelli, N.; Yin, W.; Reilly, D.; Speliotes, E.; Fox, C. S.; Hveem, K.; Holmen, O. L.; Nikpay, M.; Farlow, D. N.; Assimes, T. L.; Franceschini, N.; Robinson, J.; North, K. E.; Martin, L. W.; DePristo, M.; Gupta, N.; Escher, S. A.; Jansson, J. H.; Van Zuydam, N.; Palmer, C. N.; Wareham, N.; Koch, W.; Meitinger, T.; Peters, A.; Lieb, W.; Erbel, R.; Konig, I. R.; Kruppa, J.; Degenhardt, F.; Gottesman, O.; Bottinger, E. P.; O'Donnell, C. J.; Psaty, B. M.; Ballantyne, C. M.; Abecasis, G.; Ordovas, J. M.; Melander, O.; Watkins, H.; Orho-Melander, M.; Ardisino, D.; Loos, R. J.; McPherson, R.; Willer, C. J.; Erdmann, J.; Hall, A. S.; Samani, N. J.; Deloukas, P.; Schunkert, H.; Wilson, J. G.; Kooperberg, C.; Rich, S. S.; Tracy, R. P.; Lin, D. Y.; Altschuler, D.; Gabriel, S.; Nickerson, D. A.; Jarvik, G. P.; Cupples, L. A.; Reiner, A. P.; Boerwinkle, E.; Kathiresan, S. Loss-of-function mutations in APOC3, triglycerides, and coronary disease. *N. Engl. J. Med.* **2014**, *371* (1), 22–31.
- (5) (a) Bell, D. A.; Hooper, A. J.; Burnett, J. R. Mipomersen, an antisense apolipoprotein B synthesis inhibitor. *Expert Opin. Invest. Drugs* **2011**, *20* (2), 265–272. (b) Cuchel, M.; Rader, D. J. Microsomal transfer protein inhibition in humans. *Curr. Opin. Lipidol.* **2013**, *24* (3), 246–250.
- (6) Yen, C. L.; Stone, S. J.; Koliwad, S.; Harris, C.; Farese, R. V., Jr. Thematic review series: glycerolipids. DGAT enzymes and triacylglycerol biosynthesis. *J. Lipid Res.* **2008**, *49* (11), 2283–2301.
- (7) (a) Zammit, V. A. Hepatic triacylglycerol synthesis and secretion: DGAT2 as the link between glycaemia and triglyceridaemia. *Biochem. J.* **2013**, *451* (1), 1–12. (b) Turchetto-Zolet, A. C.; Maraschin, F. S.; de Moraes, G. L.; Cagliari, A.; Andrade, C. M.; Margis-Pinheiro, M.; Margis, R. Evolutionary view of acyl-CoA diacylglycerol acyltransferase (DGAT), a key enzyme in neutral lipid biosynthesis. *BMC Evol. Biol.* **2011**, *11*, 263.
- (8) (a) Cases, S.; Stone, S. J.; Zhou, P.; Yen, E.; Tow, B.; Lardizabal, K. D.; Voelker, T.; Farese, R. V., Jr. Cloning of DGAT2, a second mammalian diacylglycerol acyltransferase, and related family members. *J. Biol. Chem.* **2001**, *276* (42), 38870–38876. (b) Yen, C. L. E.; Monetti, M.; Burri, B. J.; Farese, R. V., Jr. The triacylglycerol synthesis enzyme DGAT1 also catalyzes the synthesis of diacylglycerols, waxes, and retinyl esters. *J. Lipid Res.* **2005**, *46* (7), 1502–1511.
- (9) (a) Devita, R. J.; Pinto, S. Current Status of the Research and Development of Diacylglycerol O-Acyltransferase 1 (DGAT1) Inhibitors. *J. Med. Chem.* **2013**, *56* (24), 9820–9825. (b) Naik, R.; Obiang-Obounou, B. W.; Kim, M.; Choi, Y.; Lee, H. S.; Lee, K. Therapeutic Strategies for Metabolic Diseases: Small-Molecule Diacylglycerol Acyltransferase (DGAT) Inhibitors. *ChemMedChem* **2014**, *9* (11), 2410–2424.
- (10) (a) Denison, H.; Nilsson, C.; Lofgren, L.; Himmelmann, A.; Martensson, G.; Knutsson, M.; Al-Shurbaji, A.; Tornqvist, H.; Eriksson, J. W. Diacylglycerol acyltransferase 1 inhibition with AZD7687 alters lipid handling and hormone secretion in the gut with intolerable side effects: a randomized clinical trial. *Diabetes, Obes. Metab.* **2014**, *16* (4), 334–343. (b) Maciejewski, B. S.; LaPerle, J. L.; Chen, D.; Ghosh, A.; Zavadski, W. J.; McDonald, T. S.; Manion, T. B.; Mather, D.; Patterson, T. A.; Hanna, M.; Watkins, S.; Gibbs, E. M.; Calle, R. A.; Stepan, C. M. Pharmacological inhibition to examine the role of DGAT1 in dietary lipid absorption in rodents and humans. *Am. J. Physiol. Gastrointest. Liver Physiol.* **2013**, *304* (11), G958–G969.
- (11) A 12-week multi-center, randomized, double-blind, placebo-controlled, parallel-group adaptive design study to evaluate the efficacy on blood glucose control and safety of five doses of LCO908 (2, 5, 10, 15 and 20 mg) or sitagliptin 100 mg on a background therapy of metformin in obese patients with type 2 diabetes. *Clinical Trial Results Database*; Novartis, 2010; <http://www.novotrd.com/ctrdWebApp/clinicaltrialrepository/displayFile.do?trialResult=4313>.
- (12) Stone, S. J.; Myers, H. M.; Watkins, S. M.; Brown, B. E.; Feingold, K. R.; Elias, P. M.; Farese, R. V., Jr. Lipopenia and skin barrier abnormalities in DGAT2-deficient mice. *J. Biol. Chem.* **2004**, *279* (12), 11767–11776.
- (13) (a) Choi, C. S.; Savage, D. B.; Kulkarni, A.; Yu, X. X.; Liu, Z. X.; Morino, K.; Kim, S.; Distefano, A.; Samuel, V. T.; Neschen, S.; Zhang, D.; Wang, A.; Zhang, X. M.; Kahn, M.; Cline, G. W.; Pandey, S. K.; Geisler, J. G.; Bhanot, S.; Monia, B. P.; Shulman, G. I. Suppression of diacylglycerol acyltransferase-2 (DGAT2), but not DGAT1, with antisense oligonucleotides reverses diet-induced hepatic steatosis and insulin resistance. *J. Biol. Chem.* **2007**, *282* (31), 22678–22688. (b) Liu, Y.; Millar, J. S.; Cromley, D. A.; Graham, M.; Crooke, R.; Billheimer, J. T.; Rader, D. J. Knockdown of acyl-CoA:diacylglycerol acyltransferase 2 with antisense oligonucleotide reduces VLDL TG and ApoB secretion in mice. *Biochim. Biophys. Acta, Mol. Cell Biol. Lipids* **2008**, *1781* (3), 97–104. (c) Yu, X. X.; Murray, S. F.; Pandey, S. K.; Booten, S. L.; Bao, D.; Song, X. Z.; Kelly, S.; Chen, S.; McKay, R.; Monia, B. P.; Bhanot, S. Antisense oligonucleotide reduction of DGAT2 expression improves hepatic steatosis and hyperlipidemia in obese mice. *Hepatology* **2005**, *42* (2), 362–371.
- (14) (a) Kim, M. O.; Lee, S.; Choi, K.; Lee, S.; Kim, H.; Kang, H.; Choi, M.; Kwon, E. B.; Kang, M. J.; Kim, S.; Lee, H.-J.; Lee, H. S.; Kwak, Y.-S.; Cho, S. Discovery of a Novel Class of Diacylglycerol Acyltransferase 2 Inhibitors with a 1H-Pyrrolo[2,3-b]Pyridine Core. *Biol. Pharm. Bull.* **2014**, *37* (10), 1655–1660. (b) Lee, K.; Kim, M.; Lee, B.; Goo, J.; Kim, J.; Naik, R.; Seo, J. H.; Kim, M. O.; Byun, Y.; Song, G. Y.; Lee, H. S.; Choi, Y. Discovery of indolyl acrylamide derivatives as human diacylglycerol acyltransferase-2 selective inhibitors. *Org. Biomol. Chem.* **2013**, *11* (5), 849–858. (c) Kim, M. O.; Lee, S. U.; Lee, H. J.; Choi, K.; Kim, H.; Lee, S.; Oh, S. J.; Kim, S.; Kang, J. S.; Lee, H. S.; Kwak, Y. S.; Cho, S. Identification and validation of a selective small molecule inhibitor targeting the diacylglycerol acyltransferase 2 activity. *Biol. Pharm. Bull.* **2013**, *36* (7), 1167–1173. (d) Wurie, H. R.; Buckett, L.; Zammit, V. A. Diacylglycerol acyltransferase 2 acts upstream of diacylglycerol acyltransferase 1 and utilizes nascent diglycerides and de novo synthesized fatty acids in HepG2 cells. *FEBS J.* **2012**, *279* (17), 3033–3047. (e) Qi, J.; Lang, W.; Geisler, J. G.; Wang, P.; Petrounia, I.; Mai, S.; Smith, C.; Askari, H.; Struble, G. T.; Williams, R.; Bhanot, S.; Monia, B. P.; Bayoumy, S.; Grant, E.; Caldwell, G. W.; Todd, M. J.; Liang, Y.; Gaul, M. D.; Demarest, K. T.; Connelly, M. A. The use of stable isotope-labeled glycerol and oleic acid to differentiate the hepatic functions of DGAT1 and -2. *J. Lipid Res.* **2012**, *53* (6), 1106–1116.
- (15) During the preparation of this manuscript, a patent application was published by Eli Lilly on pyrimidine-based DGAT2 inhibitors showing in vivo pharmacology in rodent models. Camp, N. P.; Naik, M. Novel DGAT2 inhibitors. PCT Int. Appl. WO2015077299, 2015.
- (16) Yang, D.; Fokas, D.; Li, J.; Yu, L.; Baldino, C. M. A Versatile Method for the Synthesis of Benzimidazoles from o-Nitroanilines and Aldehydes in One Step via a Reductive Cyclization. *Synthesis* **2005**, *1*, 47–56.

- (17) (a) Ivanova, N. V.; Sviridov, S. I.; Stepanov, A. E. Parallel solution-phase synthesis of substituted 2-(1,2,4-triazol-3-yl)-benzimidazoles. *Tetrahedron Lett.* **2006**, *47* (46), 8025–8027. (b) Lin, S.; Yang, L. A simple and efficient procedure for the synthesis of benzimidazoles using air as the oxidant. *Tetrahedron Lett.* **2005**, *46* (25), 4315–4319.
- (18) Lin, S.-Y.; Isome, Y.; Stewart, E.; Liu, J.-F.; Yohannes, D.; Yu, L. Microwave-assisted one step high-throughput synthesis of benzimidazoles. *Tetrahedron Lett.* **2006**, *47* (17), 2883–2886.
- (19) Guillaume, D.; Brum-Bousquet, M.; Aitken, D. J.; Husson, H.-P. Cyclopropanation of dibenylaminoacetonitrile: evaluation of 1,2-dibromides and cyclic 1,2-sulfates as dielectrophiles. *Bull. Soc. Chim. Fr.* **1994**, *131*, 391–396.
- (20) (a) McFie, P. J.; Stone, S. J. A fluorescent assay to quantitatively measure in vitro acyl CoA:diacylglycerol acyltransferase activity. *J. Lipid Res.* **2011**, *52* (9), 1760–1764. (b) Harris, C. A.; Haas, J. T.; Streeper, R. S.; Stone, S. J.; Kumari, M.; Yang, K.; Han, X.; Brownell, N.; Gross, R. W.; Zechner, R.; Farese, R. V., Jr. DGAT enzymes are required for triacylglycerol synthesis and lipid droplets in adipocytes. *J. Lipid Res.* **2011**, *52* (4), 657–667. (c) Cao, J.; Cheng, L.; Shi, Y. Catalytic properties of MGAT3, a putative triacylglycerol synthase. *J. Lipid Res.* **2007**, *48* (3), 583–591. (d) Yen, C. L.; Farese, R. V., Jr. MGAT2, a monoacylglycerol acyltransferase expressed in the small intestine. *J. Biol. Chem.* **2003**, *278* (20), 18532–18537. (e) Yen, C. L.; Stone, S. J.; Cases, S.; Zhou, P.; Farese, R. V., Jr. Identification of a gene encoding MGAT1, a monoacylglycerol acyltransferase. *Proc. Natl. Acad. Sci. U. S. A.* **2002**, *99* (13), 8512–8517.
- (21) More details on the in vitro assay development and mechanistic characterizations of DGAT2 inhibitors will be published in the future.
- (22) (a) Shultz, M. D. Setting expectations in molecular optimizations: Strengths and limitations of commonly used composite parameters. *Bioorg. Med. Chem. Lett.* **2013**, *23* (21), 5980–5991. (b) Freeman-Cook, K. D.; Hoffman, R. L.; Johnson, T. W. Lipophilic efficiency: the most important efficiency metric in medicinal chemistry. *Future Med. Chem.* **2013**, *5* (2), 113–115. (c) Tarcsay, A.; Nyiri, K.; Keseru, G. M. Impact of Lipophilic Efficiency on Compound Quality. *J. Med. Chem.* **2012**, *55* (3), 1252–1260. (d) Leeson, P. D.; Empfield, J. R. Reducing the risk of drug attrition associated with physicochemical properties. *Annu. Rep. Med. Chem.* **2010**, *45*, 393–407. (e) Edwards, M. P.; Price, D. A. Role of Physicochemical Properties and Ligand Lipophilicity Efficiency in Addressing Drug Safety Risks. *Annu. Rep. Med. Chem.* **2010**, *45*, 380–391.
- (23) Lombardo, F.; Shalaeva, M. Y.; Tupper, K. A.; Gao, F. ElogD(oct): a tool for lipophilicity determination in drug discovery. 2. Basic and neutral compounds. *J. Med. Chem.* **2001**, *44* (15), 2490–2497.
- (24) (a) Di, L.; Keefer, C.; Scott, D. O.; Strelevitz, T. J.; Chang, G.; Bi, Y. A.; Lai, Y.; Duckworth, J.; Fenner, K.; Troutman, M. D.; Obach, R. S. Mechanistic insights from comparing intrinsic clearance values between human liver microsomes and hepatocytes to guide drug design. *Eur. J. Med. Chem.* **2012**, *57*, 441–448. (b) Walsky, R. L.; Bauman, J. N.; Bourcier, K.; Giddens, G.; Lapham, K.; Negahban, A.; Ryder, T. F.; Obach, R. S.; Hyland, R.; Goosen, T. C. Optimized assays for human UDP-glucuronosyltransferase (UGT) activities: altered alamethicin concentration and utility to screen for UGT inhibitors. *Drug Metab. Dispos.* **2012**, *40* (5), 1051–1065. (c) Gill, K. L.; Houston, J. B.; Galetin, A. Characterization of in vitro glucuronidation clearance of a range of drugs in human kidney microsomes: comparison with liver and intestinal glucuronidation and impact of albumin. *Drug Metab. Dispos.* **2012**, *40* (4), 825–835. (d) Kilford, P. J.; Stringer, R.; Sohal, B.; Houston, J. B.; Galetin, A. Prediction of drug clearance by glucuronidation from in vitro data: use of combined cytochrome P450 and UDP-glucuronosyltransferase cofactors in alamethicin-activated human liver microsomes. *Drug Metab. Dispos.* **2009**, *37* (1), 82–89. (e) Rowland, A.; Knights, K. M.; Mackenzie, P. I.; Miners, J. O. The "albumin effect" and drug glucuronidation: bovine serum albumin and fatty acid-free human serum albumin enhance the glucuronidation of UDP-glucuronosyltransferase (UGT) 1A9 substrates but not UGT1A1 and UGT1A6 activities. *Drug Metab. Dispos.* **2008**, *36* (6), 1056–1062.
- (25) Kaiyosaaari, S.; Finel, M.; Koskinen, M. N-glucuronidation of drugs and other xenobiotics by human and animal UDP-glucuronosyltransferases. *Xenobiotica* **2011**, *41* (8), 652–669.
- (26) Lovering, F. Escape from Flatland 2: complexity and promiscuity. *MedChemComm* **2013**, *4* (3), 515–519.
- (27) Rose, K.; Yang, Y.-S.; Sciotti, R.; Cai, H. Structure-activity relationship (SAR): effort towards blocking N-glucuronidation of indazoles (PF-03376056) by human UGT1A enzymes. *Drug Metab. Lett.* **2009**, *3* (1), 28–34.
- (28) A subset of analogues of compounds **8** and **9** that incorporate other substituents at 4 position of the pyrazole ring, such as cyano, methyl, cyclopropyl, or trifluoromethyl, showed no improvement of potency and LipE over compound **8** and **9** among tested, while showing measurable metabolic turnover in HLM.
- (29) Dow, R. L.; Li, J.-C.; Pence, M. P.; Gibbs, E. M.; LaPerle, J. L.; Litchfield, J.; Piotrowski, D. W.; Munchhof, M. J.; Manion, T. B.; Zavadoski, W. J.; Walker, G. S.; McPherson, R. K.; Tapley, S.; Sugarman, E.; Guzman-Perez, A.; DaSilva-Jardine, P. Discovery of PF-04620110, a Potent, Selective, and Orally Bioavailable Inhibitor of DGAT-1. *ACS Med. Chem. Lett.* **2011**, *2* (5), 407–412.
- (30) Ishibashi, S.; Brown, M. S.; Goldstein, J. L.; Gerard, R. D.; Hammer, R. E.; Herz, J. Hypercholesterolemia in low density lipoprotein receptor knockout mice and its reversal by adenovirus-mediated gene delivery. *J. Clin. Invest.* **1993**, *92* (2), 883–893.
- (31) Cuchel, M.; Bloedon, L. T.; Szapary, P. O.; Kolansky, D. M.; Wolfe, M. L.; Sarkis, A.; Millar, J. S.; Ikewaki, K.; Siegelman, E. S.; Gregg, R. E.; Rader, D. J. Inhibition of microsomal triglyceride transfer protein in familial hypercholesterolemia. *N. Engl. J. Med.* **2007**, *356* (2), 148–156.
- (32) PF-06424439 is commercially available from Sigma Aldrich (catalogue number PZ0233).
- (33) Gerdes, L. U.; Gerdes, C.; Klausen, I. C.; Faergeman, O. Generation of analytic plasma lipoprotein profiles using two prepacked superose 6B columns. *Clin. Chim. Acta* **1992**, *205* (1–2), 1–9.
- (34) Folch, J.; Lees, M.; Sloane Stanley, G. H. A simple method for the isolation and purification of total lipides from animal tissues. *J. Biol. Chem.* **1957**, *226* (1), 497–509.
- (35) Kaluzny, M. A.; Duncan, L. A.; Merritt, M. V.; Epps, D. E. Rapid separation of lipid classes in high yield and purity using bonded phase columns. *J. Lipid Res.* **1985**, *26* (1), 135–140.
- (36) El-Hamdy, A. H.; Christie, W. W. Separation of non-polar lipids by high performance liquid chromatography on a cyanopropyl column. *J. High Resolut. Chromatogr.* **1993**, *16* (1), 55–57.